The Multi Level Multi Domain method (MLMD) for Particle In Cell plasma simulations

presenter: M.E. Innocenti[1]

S. Markidis[2], G. Lapenta[1] and the iPic3D team

1: Centre for Plasma Astrophysics, KULeuven, Belgium
2: HPCViz Department, KTH Royal Institute of Technology, Stockholm, Sweden

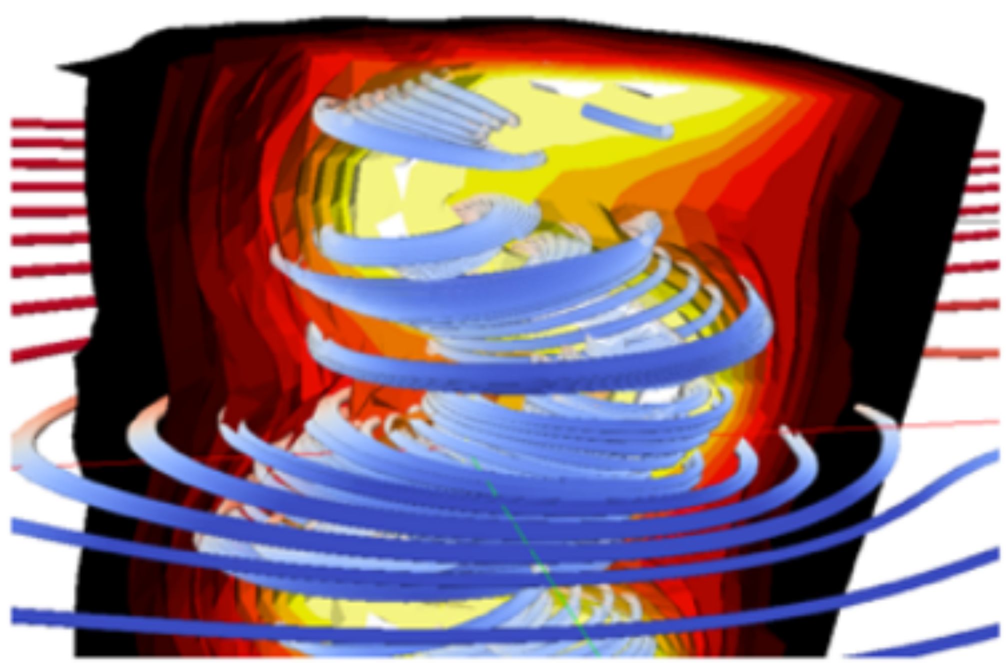

WORKSHOP "COMPUTATIONAL SOLAR AND ASTROPHYSICAL MODELING"
Juelich, September 14-18, 2015

Outline

- P1: motivations: beyond the Implicit Moment Method
- P2: the Multi-Level Multi-Domain (MLMD) method
- P3: collisionless magnetic reconnection: the essential facts
- P4: MLMD simulations of collisionless magnetic reconnection
- P5: MLMD simulations of turbulence
- P6: conclusions

P1: Sample of the physical problems tackled with the Implicit Moment Method (IMM) code iPic3D

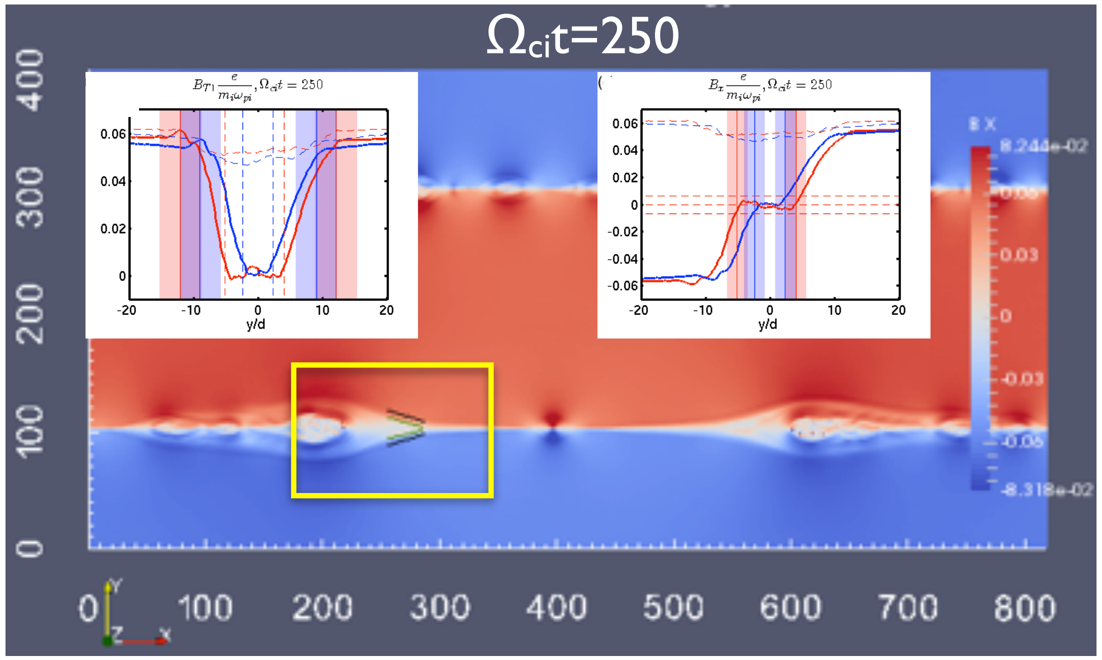

Magnetic field switch-off in PIC simulations of collisionless magnetic reconnection with guide field
M.E. Innocenti et al.

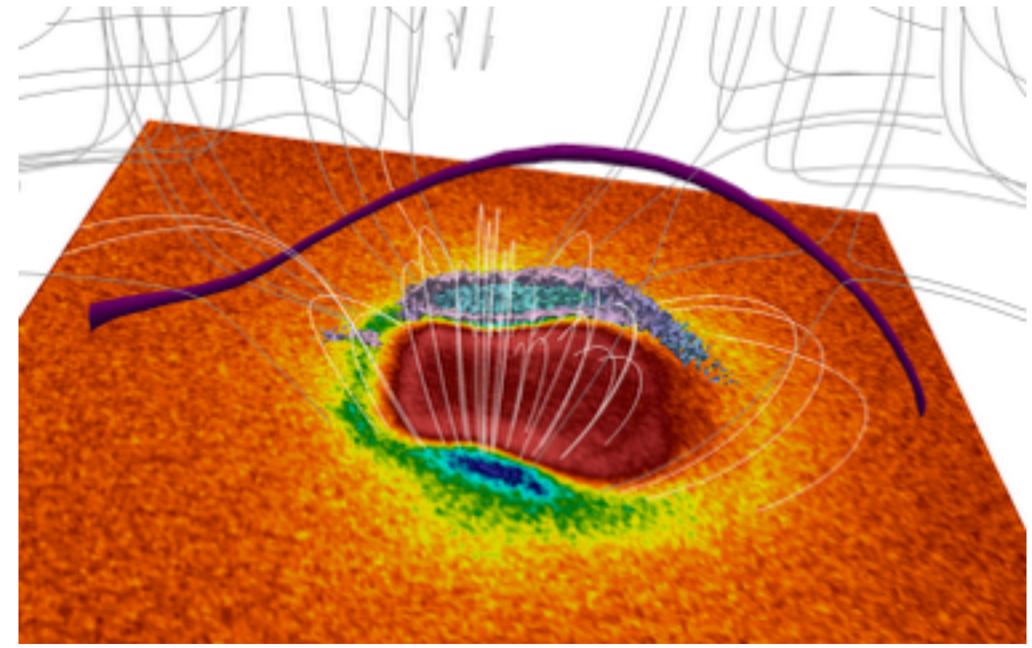

Solar wind - Lunar Magnetic Anomaly interaction
J. Deca et al.

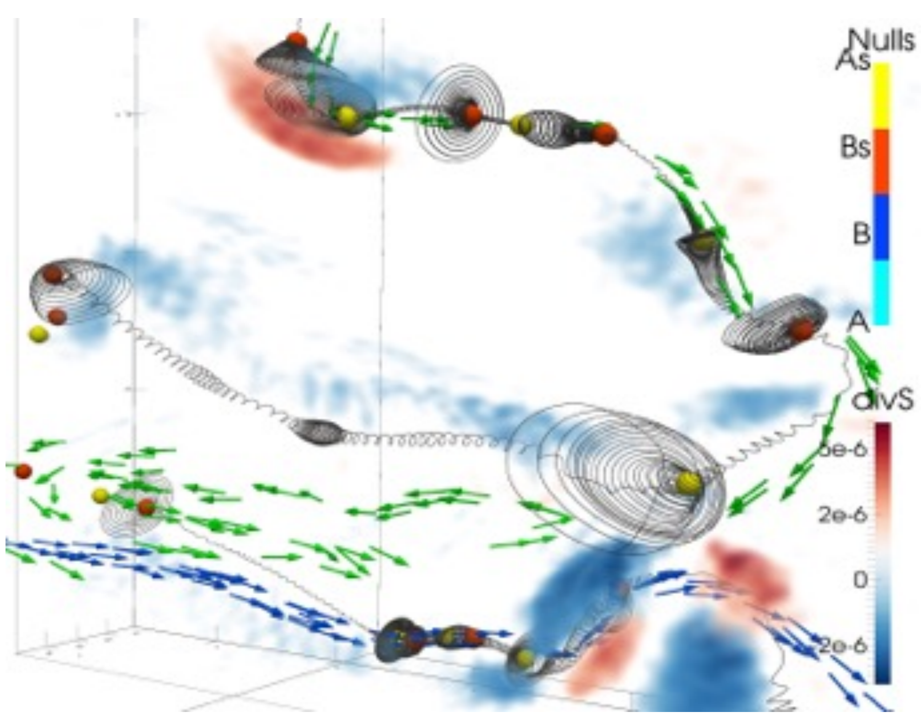

Topology of magnetic null points and associated energy dissipation patterns
V. Olshevskyi et al.

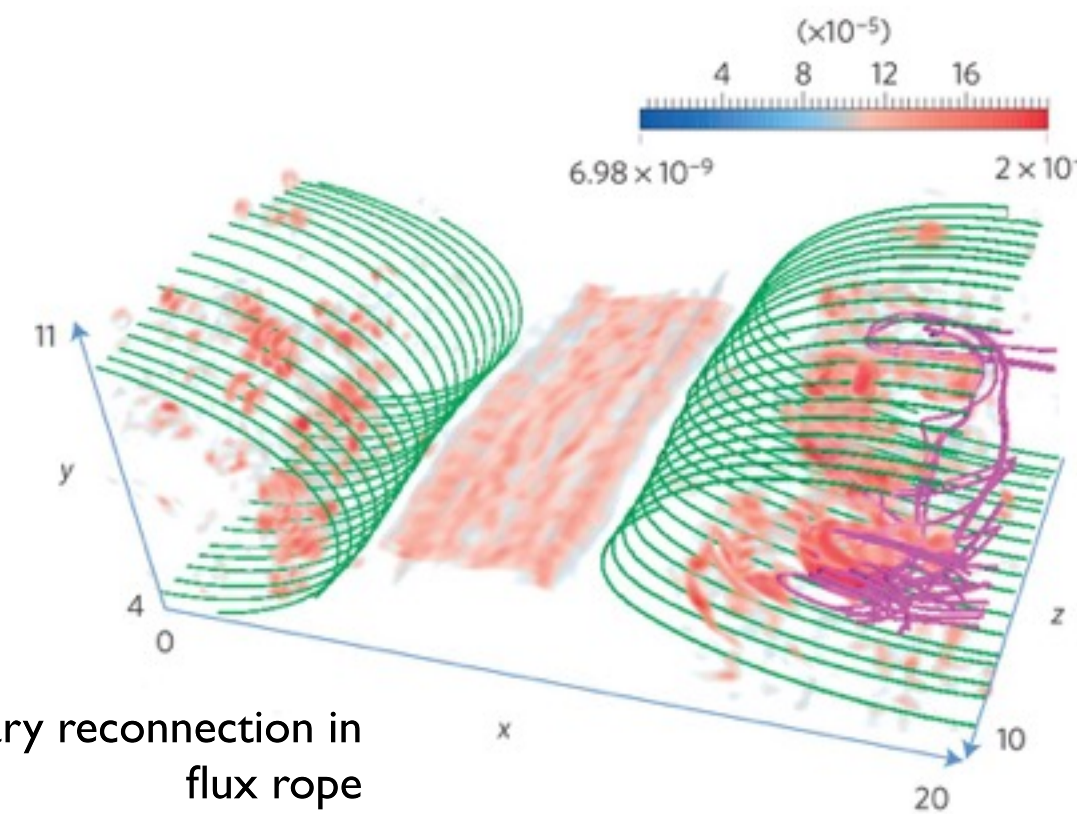

Secondary reconnection in flux rope
Lapenta et al. -Nature

Markidis et al., 2010

P1: Sample of the physical problems tackled with the Implicit Moment Method (IMM) code iPic3D

What do these simulations have in common?

computational cost ~10^5-10^6 core hours, a significant fraction of a standard PRACE Tier 0 allocation

PRACE: pan-European supercomputing infrastructure

top 500 list (June 2015)

RANK	SITE	SYSTEM	CORES	RMAX (TFLOP/S)	RPEAK (TFLOP/S)	POWER (KW)
1	National Super Computer Center in Guangzhou China	**Tianhe-2 (MilkyWay-2)** - TH-IVB-FEP Cluster, Intel Xeon E5-2692 12C 2.200GHz, TH Express-2, Intel Xeon Phi 31S1P NUDT	3,120,000	33,862.7	54,902.4	17,808
2	DOE/SC/Oak Ridge National Laboratory United States	**Titan** - Cray XK7 , Opteron 6274 16C 2.200GHz, Cray Gemini interconnect, NVIDIA K20x Cray Inc.	560,640	17,590.0	27,112.5	8,209
3	DOE/NNSA/LLNL United States	**Sequoia** - BlueGene/Q, Power BQC 16C 1.60 GHz, Custom IBM	1,572,864	17,173.2	20,132.7	7,890
4	RIKEN Advanced Institute for Computational Science (AICS) Japan	K computer, SPARC64 VIIIfx 2.0GHz, Tofu interconnect Fujitsu	705,024	10,510.0	11,280.4	12,660
5	DOE/SC/Argonne National Laboratory United States	**Mira** - BlueGene/Q, Power BQC 16C 1.60GHz, Custom IBM	786,432	8,586.6	10,066.3	3,945
6	Swiss National Supercomputing Centre (CSCS) Switzerland	**Piz Daint** - Cray XC30, Xeon E5-2670 8C 2.600GHz, Aries interconnect , NVIDIA K20x Cray Inc.	115,984	6,271.0	7,788.9	2,325
7	King Abdullah University of Science and Technology Saudi Arabia	**Shaheen II** - Cray XC40, Xeon E5-2698v3 16C 2.3GHz, Aries interconnect Cray Inc.	196,608	5,537.0	7,235.2	2,834
8	Texas Advanced Computing Center/Univ. of Texas United States	**Stampede** - PowerEdge C8220, Xeon E5-2680 8C 2.700GHz, Infiniband FDR, Intel Xeon Phi SE10P Dell	462,462	5,168.1	8,520.1	4,510
9	Forschungszentrum Juelich (FZJ) Germany	**JUQUEEN** - BlueGene/Q, Power BQC 16C 1.600GHz, Custom Interconnect IBM	458,752	5,008.9	5,872.0	2,301

P1: Which are the "expensive" phases of an iPic3D simulation?

schematics of an iPic3D simulations

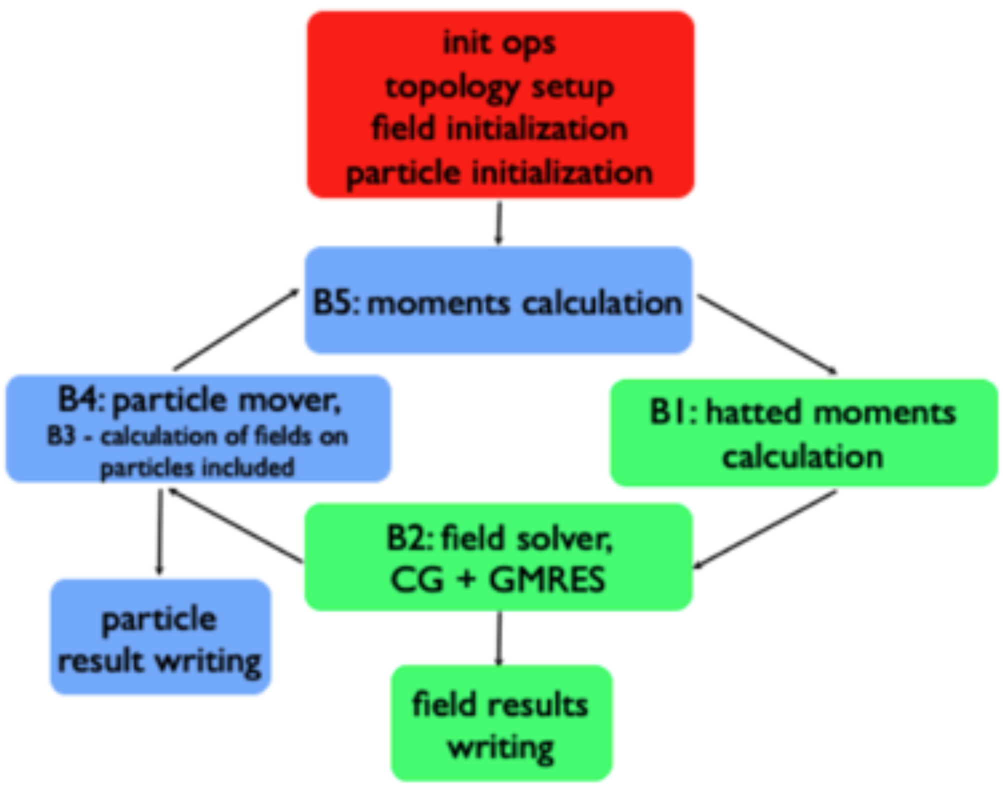

operations on grid points

operations on particles

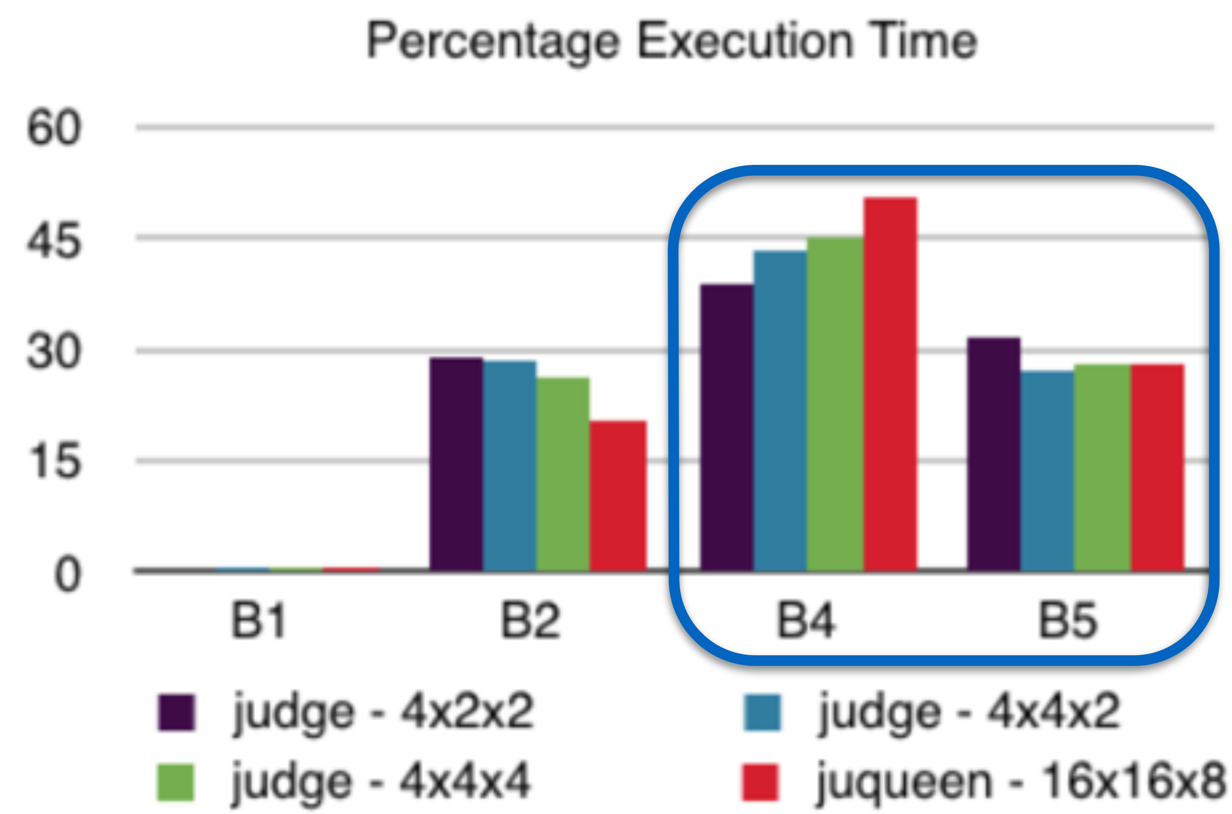

Scalasca profiling with different input parameters:
most of the simulation time is spent in particle- related operations

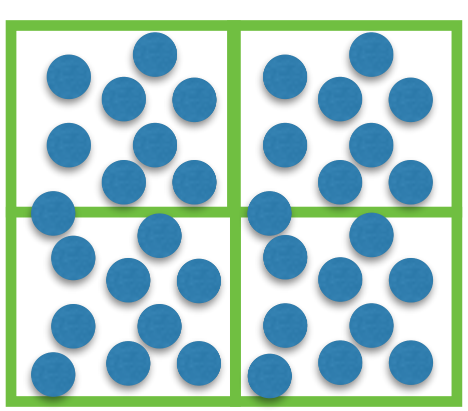

Np >> Ng
"particle dominated" regimes
Np: particle #
Ng: grid points #

Why is the number of particles high?

- numerical noise proportional to $1/\sqrt{Np}$ → minimum number of particles per cell to be kept
- large domains to be simulated with high spatial resolutions → high Ng → high Np
- Np is proportional to $(m_i/m_e)^{D/2}$, with m_i/m_e mass ratio and D problem dimensionality (with fixed ion scale domain size, fixed electron scale resolution and increasing mass ratio between particle species)

P1: Which are the "expensive" phases of an iPic3D simulation?

schematics of an iPic3D simulations

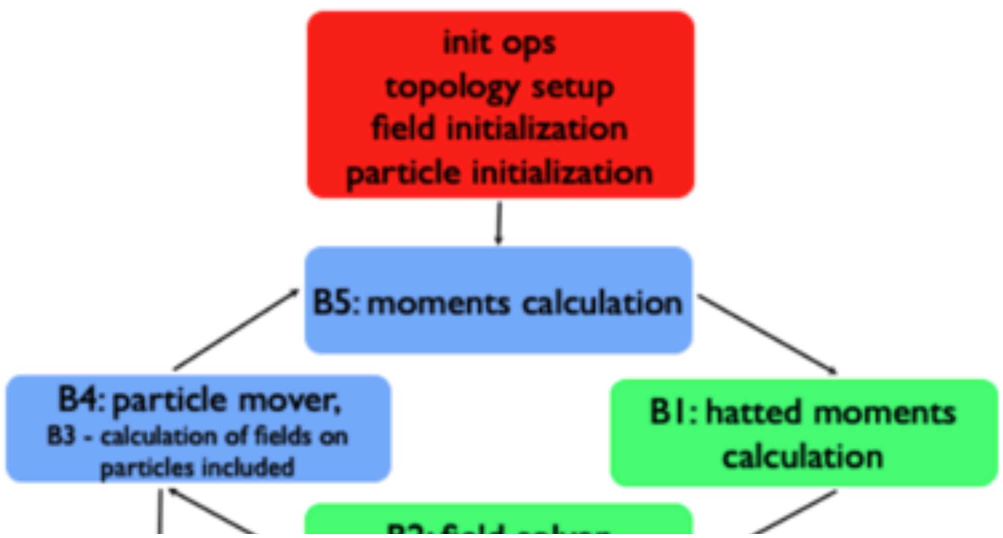

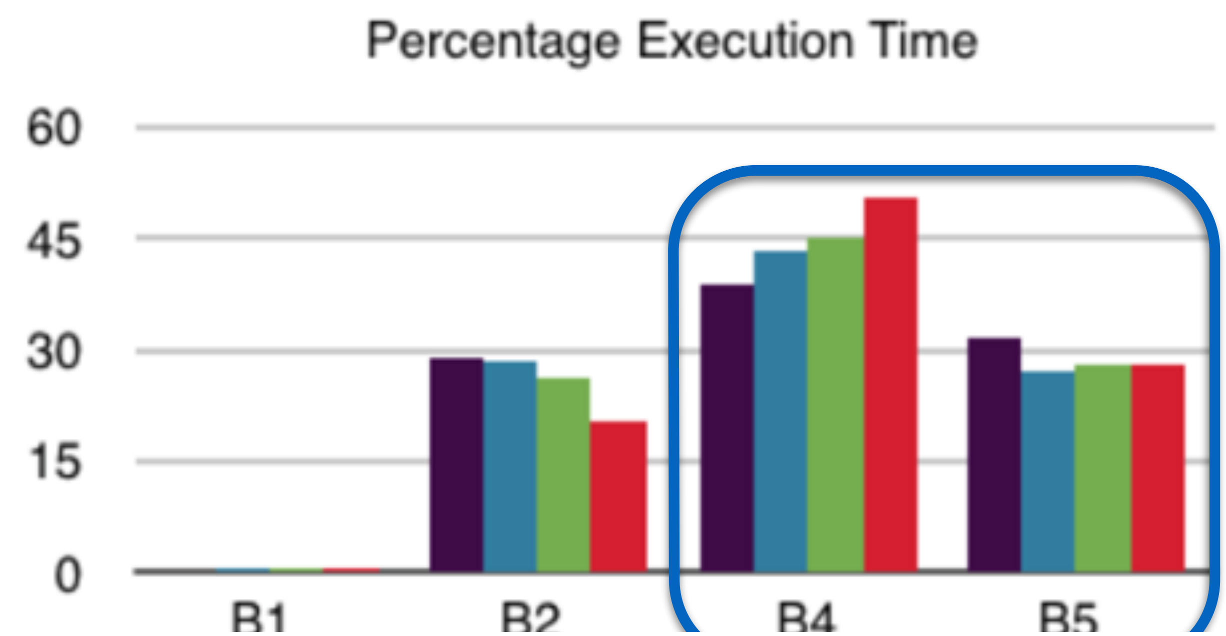

even if the Implicit Moment Method is used,
advanced techniques are needed to further reduce simulation costs
→ adaptive mesh techniques

most of the simulation time is spent in particle- related operations

operations on grid points

operations on particles

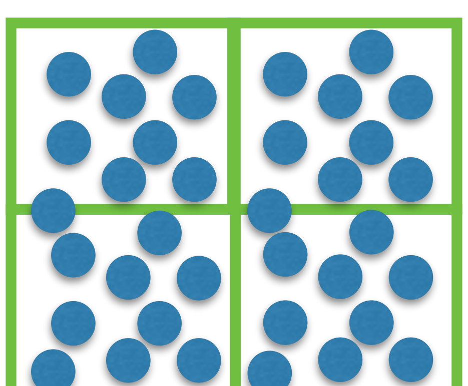

Np >> Ng
"particle dominated" regimes
Np: particle #
Ng: grid points #

Why is the number of particles high?

- numerical noise proportional to 1/ √Np → minimum number of particles per cell to be kept
- large domains to be simulated with high spatial resolutions → high Ng → high Np
- Np is proportional to $(m_i/m_e)^{D/2}$, with m_i/m_e mass ratio and D problem dimensionality (with fixed ion scale domain size, fixed electron scale resolution and increasing mass ratio between particle species)

P1: Adaptive techniques for Particle In Cell (PIC) simulations

Moving Mesh Adaptation (MMA)

Brackbill, 1993, Delzanno 2008, Lapenta, 2011, Chacon 2011

fixed number of grid points; points are attracted in the "interesting" part of the domain, according to a monitor quantity

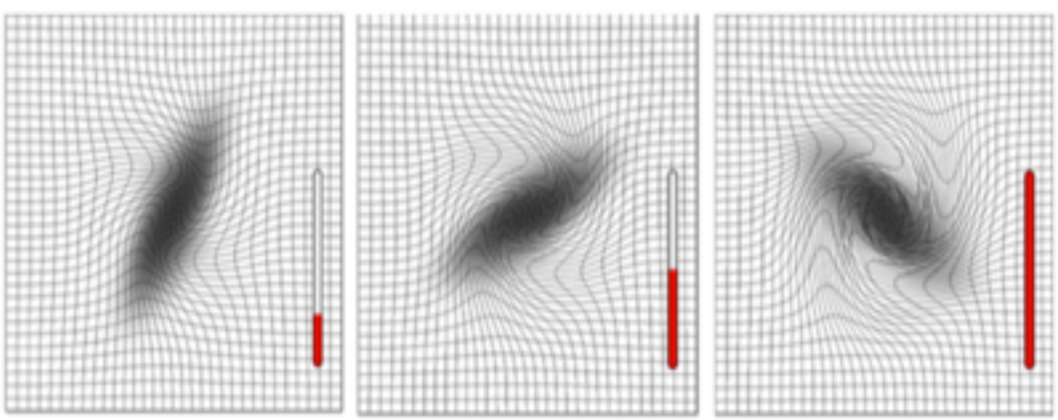

Chacon 2011

Adaptive Mesh Refinement (AMR)

Vay, 2004, Fujimoto et Sydora, 2008

changing number of grid points; cells are split or coalesced, according to a monitor quantity; all existing AMR codes are explicit

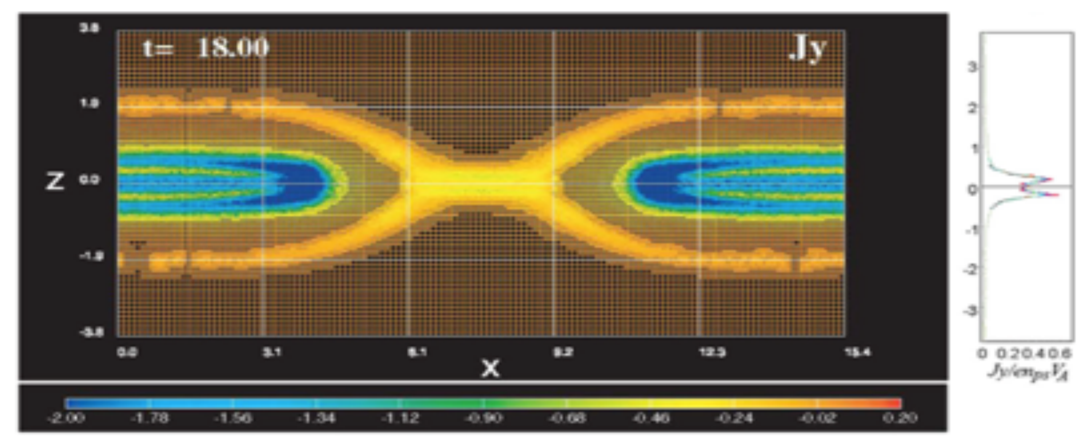

Fujimoto 2008

Multi-Level Multi-Domain (MLMD)

Innocenti, 2013; Beck, 2014; Innocenti, 2015

different grid levels are simulated with different spatial and temporal resolution; the IMM method is used →the advantages of the IMM and of adaptivity are harnessed together

P2: The Multi-Level Multi-Domain (MLMD) method:
a semi-implicit adaptive method for Particle In Cell plasma simulations

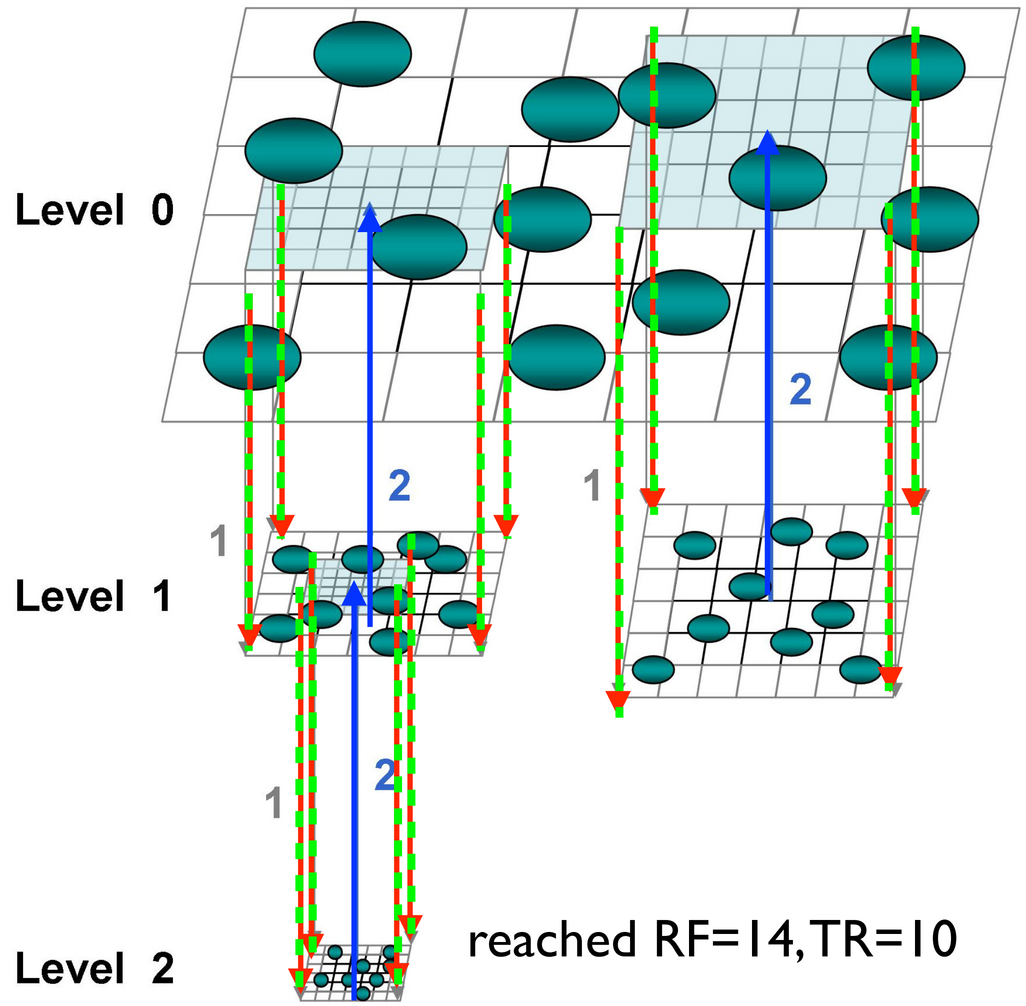

- the different levels are simulated fully with fields and particles with different spatial and temporal resolutions
  → the highest resolution is used only when needed
  → ion and (when resolved) electron processes are correctly resolved, at a much lower computational cost

- realistic mass ratios are cheaply handled: ion scale resolution on one level, electron scale resolution on the other

- the IMM grants more freedom in the choice of the local resolutions, in the limits of the stability constraint
  $0.1 < v_{th,e}\, dt/dx < 1$
  (explicit algorithms have to resolve inverse electron plasma frequency, Debye length, smaller, for stability reasons)

The MLMD terminology:

jump in *spatial* resolution: Refinement Factor RF
jump in *temporal* resolution: Time Ratio TR
lower resolution grid: Coarse Grid (CG)
higher resolution grid: Refined Grif (RG)

P2: The stability constraint of the IMM and the MLMD system

Implicit Moment Method (IMM) stability constraint

$0.1 < v_{th,e}\, dt/dx < 1$

"large" dx → Finite Grid Instability (FGI)
sampling is not frequent enough; spurious high frequencies give non-physical electric field oscillations and particle heating

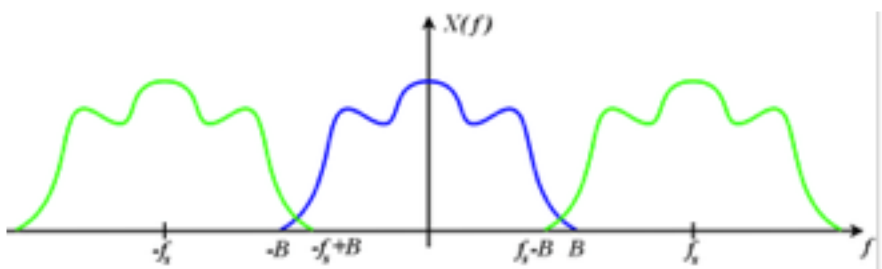

$v_{th,e}\, dt > dx$ →
assumption for Taylor expansion used in the IMM broken → inaccurate results

$$\rho^{n+\theta} = \sum_p q_p S(\mathbf{x}-\mathbf{x}^{n+\theta}) = \sum_p q_p [S(\mathbf{x}-\mathbf{x}^n) + (\mathbf{x}^{n+\theta}-\mathbf{x}^n)\nabla S(\mathbf{x}-\mathbf{x}^n) + \frac{1}{2}(\mathbf{x}^{n+\theta}-\mathbf{x}^n)^2 \nabla\nabla S(\mathbf{x}-\mathbf{x}^n) + \mathcal{O}(\mathbf{x}-\mathbf{x}^n)^3]$$

$$(\mathbf{x}^{n+\theta}-\mathbf{x}^n) = f(\mathbf{E}^{n+\theta})$$

$S(\mathbf{x}-\mathbf{x}^{n+\theta})$ particle shape function at "future" time

$S(\mathbf{x}-\mathbf{x}^n)$ particle shape function at current time

Harris field in magnetic reconnection with FGI

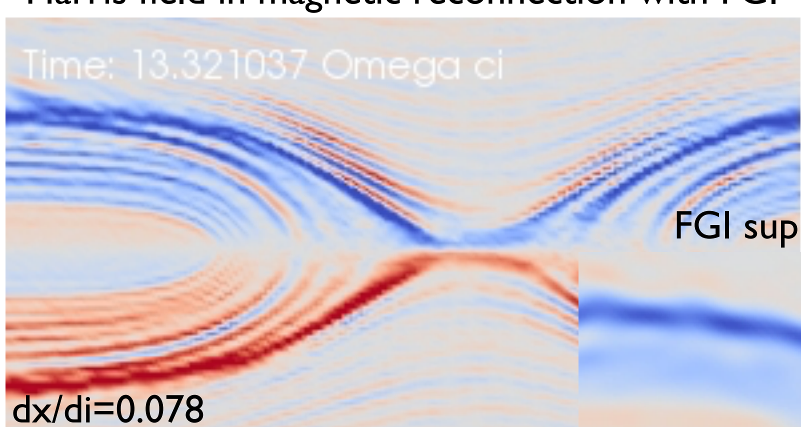

FGI can be suppressed with field smoothing!

FGI suppressed with field smoothing

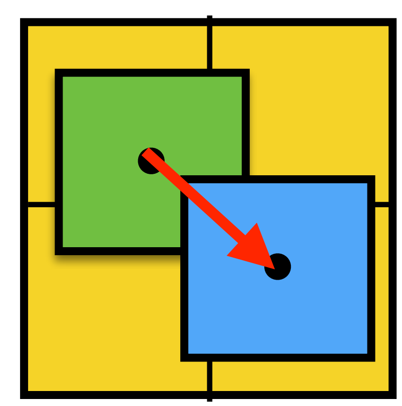

with fixed time step across the MLMD system, the Coarse Grid risks falling into this regime

with fixed time step across the MLMD system, the Refined Grid risks falling into this regime

different time steps have to be used at the different levels → temporal sub-stepping

P2: A MLMD coarse grid iteration with sub-stepping

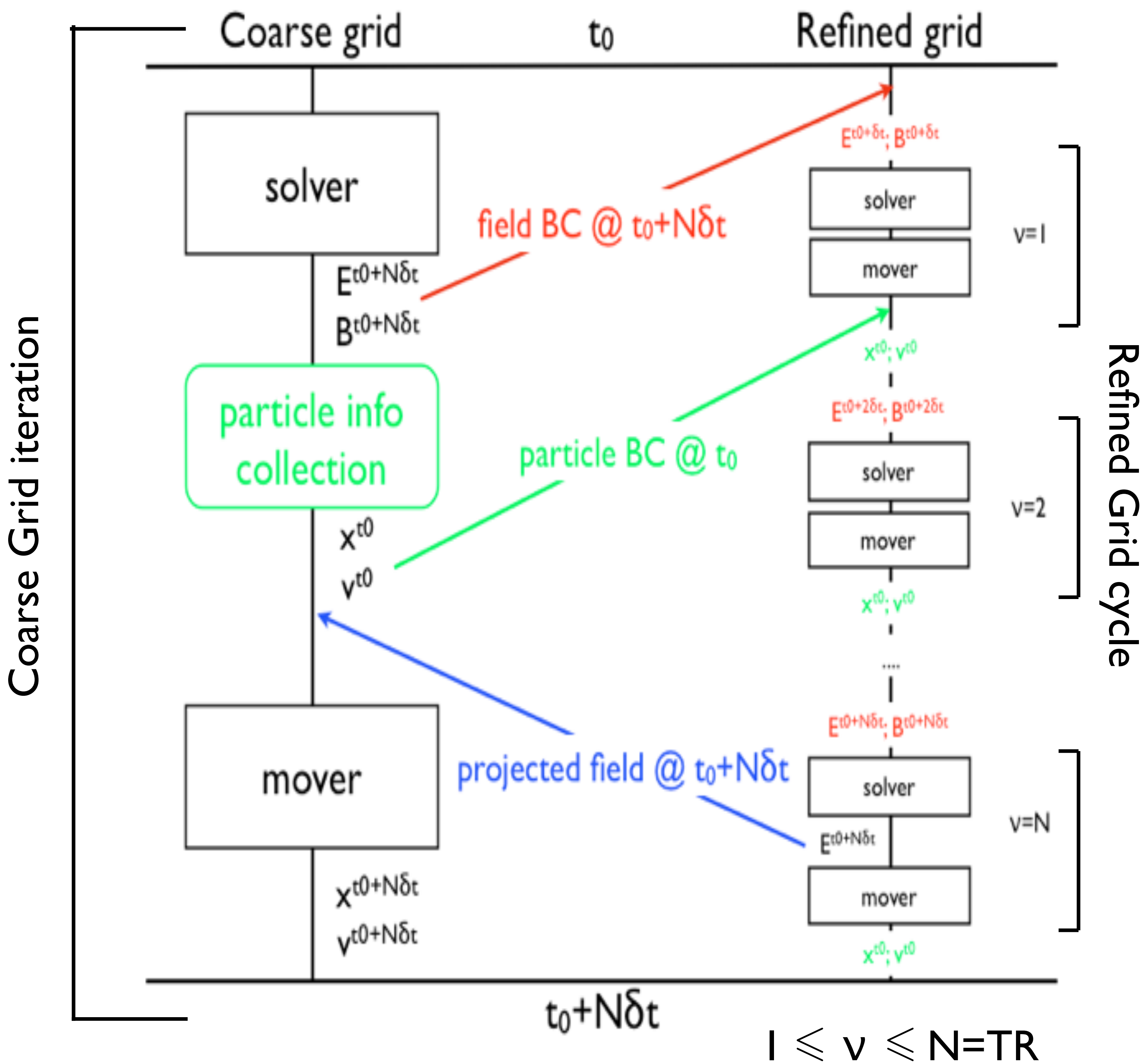

Sub-cycling allows both grids to work in an "healthier" $v_{th,e}$ dt/dx regime and to save execution time and resources; the time ratio TR is chosen from input-file

P2: Grid interlocking operations

1. Boundary condition interpolation (C2R)

$$\Xi_{I,g_{l+1}} = \sum_{g_l} \Xi_{N,g_l} W_{g_l}(\mathbf{x}_{g_l} - \mathbf{x}_{g_{l+1}})$$

W: "normal" interpolation function from PIC

2. Refined field projection (R2C)

$$\mathbf{E}_{P,g_l} = \frac{1}{2}\left(\mathbf{E}_{N,g_l} + \mathbb{P}^{g_{l+1}\to g_l}\left(\mathbf{E}_{N,g_l+1}\right)\right)$$

$$\mathbb{P}^{g_{l+1}\to g_l}\left(\mathbf{E}_{N,g_l+1}\right) = \frac{\sum_{g_{l+1}} \mathbf{E}_{N,g_{l+1}} W_{g_l}(\mathbf{x}_{g_l}-\mathbf{x}_{g_{l+1}})}{\sum_{g_{l+1}} W_{g_l}(\mathbf{x}_{g_l}-\mathbf{x}_{g_{l+1}})}$$

3. Boundary refined particle repopulation (C2R)

Coarse Level Particle

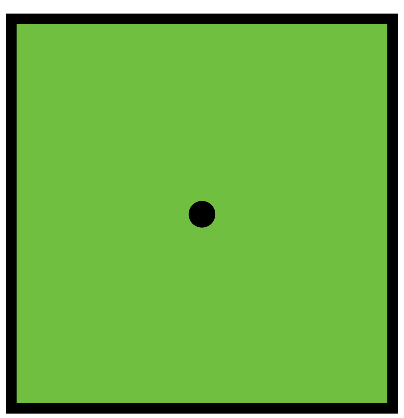

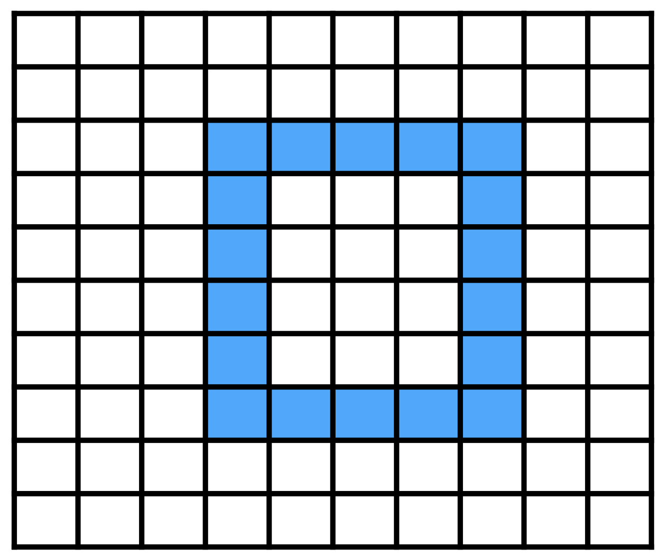

Particles sitting at the boundaries of the Refined Grid are generated according to the velocities and positions of corresponding Coarse Grid particles for consistent particle motion between CG and RG at the grid boundaries

$$\mathbf{v}_{p_{g_{l+1}}}^{t0+dt} = \mathbf{v}_{p_{g_l}}^{t0+dt}$$

$$q_{p_{g_{l+1}}}^{t0+dt} = q_{p_{g_l}}^{t0+dt} / RF^2$$

the aim is to preserve the combined particle shape function and the distribution function at the boundaries

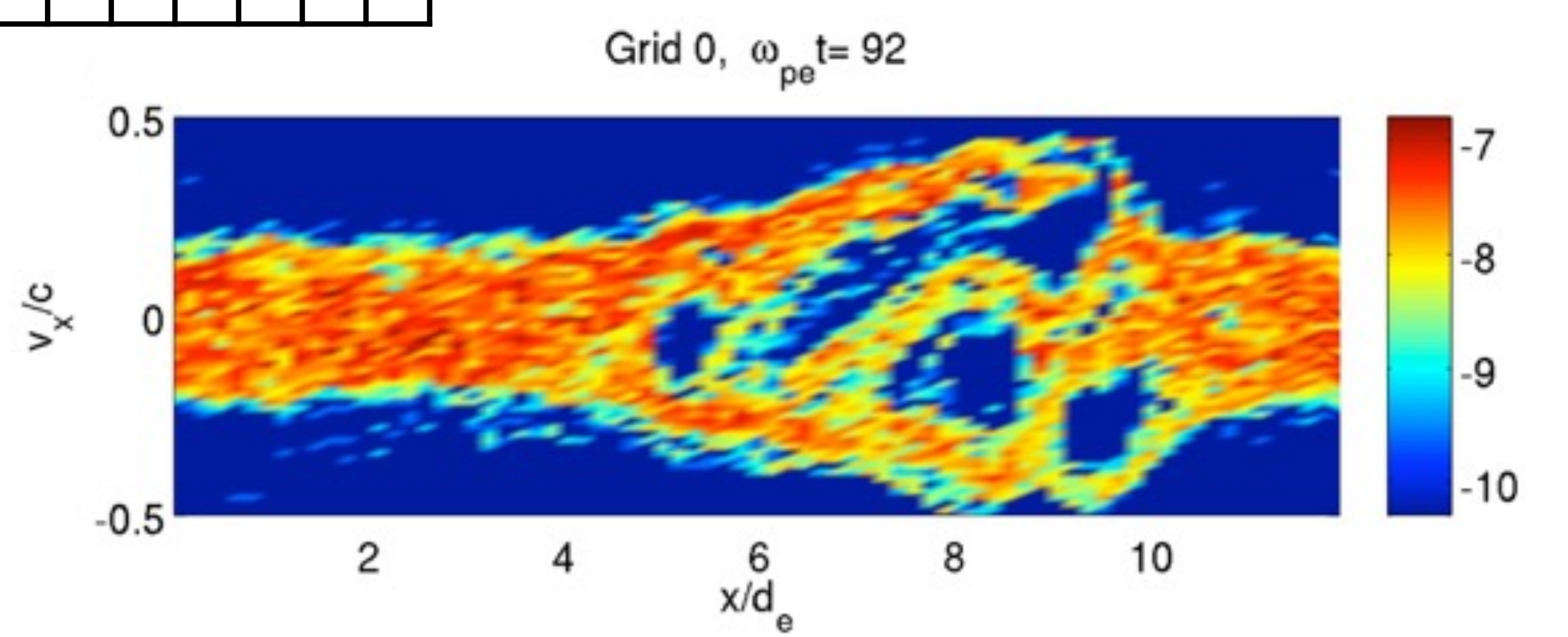

electron hole merging phase in a 1D3V MLMD two stream instability with RF=4

P2: Grid interlocking operations

1. Boundary condition interpolation (C2R)

$$\Xi_{I,g_{l+1}} = \sum_{g_l} \Xi_{N,g_l} W_{g_l}(\mathbf{x}_{g_l} - \mathbf{x}_{g_{l+1}})$$

W: "normal" interpolation function from PIC

2. Refined field projection (R2C)

$$\mathbf{E}_{P,g_l} = \frac{1}{2}\left(\mathbf{E}_{N,g_l} + \mathbb{P}^{g_{l+1}\to g_l}\left(\mathbf{E}_{N,g_{l+1}}\right)\right)$$

$$\mathbb{P}^{g_{l+1}\to g_l}\left(\mathbf{E}_{N,g_{l+1}}\right) = \frac{\sum_{g_{l+1}} \mathbf{E}_{N,g_{l+1}} W_{g_l}(\mathbf{x}_{g_l} - \mathbf{x}_{g_{l+1}})}{\sum_{g_{l+1}} W_{g_l}(\mathbf{x}_{g_l} - \mathbf{x}_{g_{l+1}})}$$

3. Boundary refined particle repopulation (C2R)

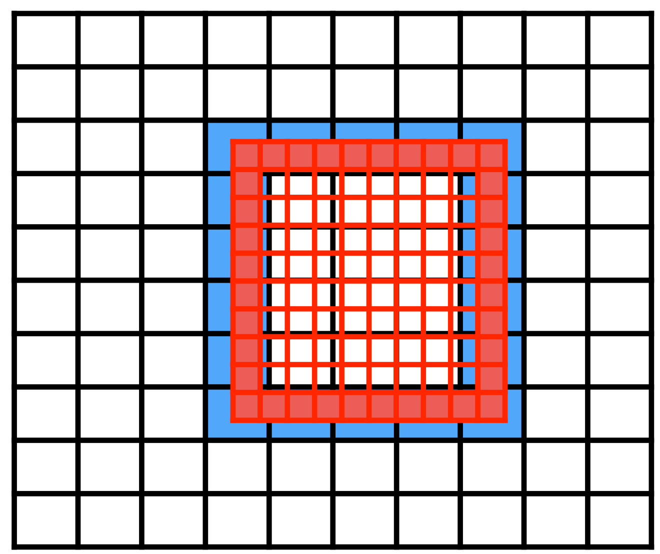

Particles sitting at the boundaries of the Refined Grid are generated according to the velocities and positions of corresponding Coarse Grid particles for consistent particle motion between CG and RG at the grid boundaries

Refined Level Particles

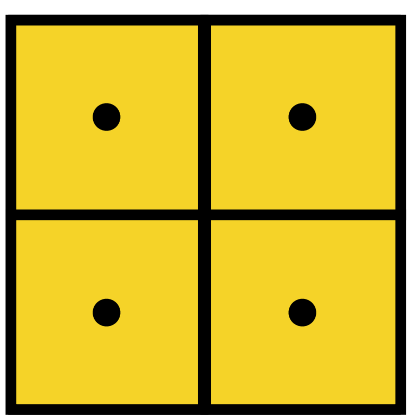

$$\mathbf{v}_{p_{g_{l+1}}}^{t0+dt} = \mathbf{v}_{p_{g_l}}^{t0+dt}$$

$$q_{p_{g_{l+1}}}^{t0+dt} = q_{p_{g_l}}^{t0+dt} / RF^2$$

the aim is to preserve the combined particle shape function and the distribution function at the boundaries

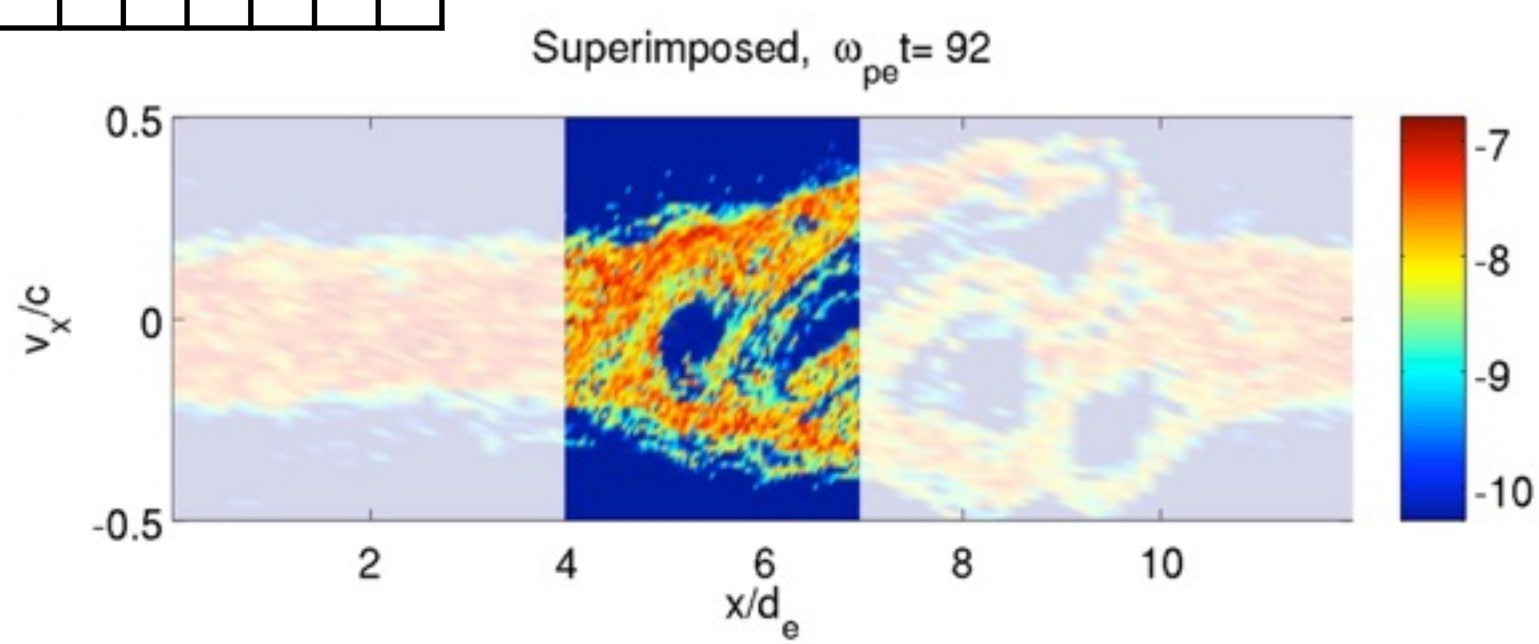

electron hole merging phase in a 1D3V MLMD two stream instability with RF=4

P2: Computing resource saving

Comparing the computing cost of MLMD simulations with single level simulations, resolved everywhere with the highest MLMD resolution

we need this resolution only in a fraction of the domain

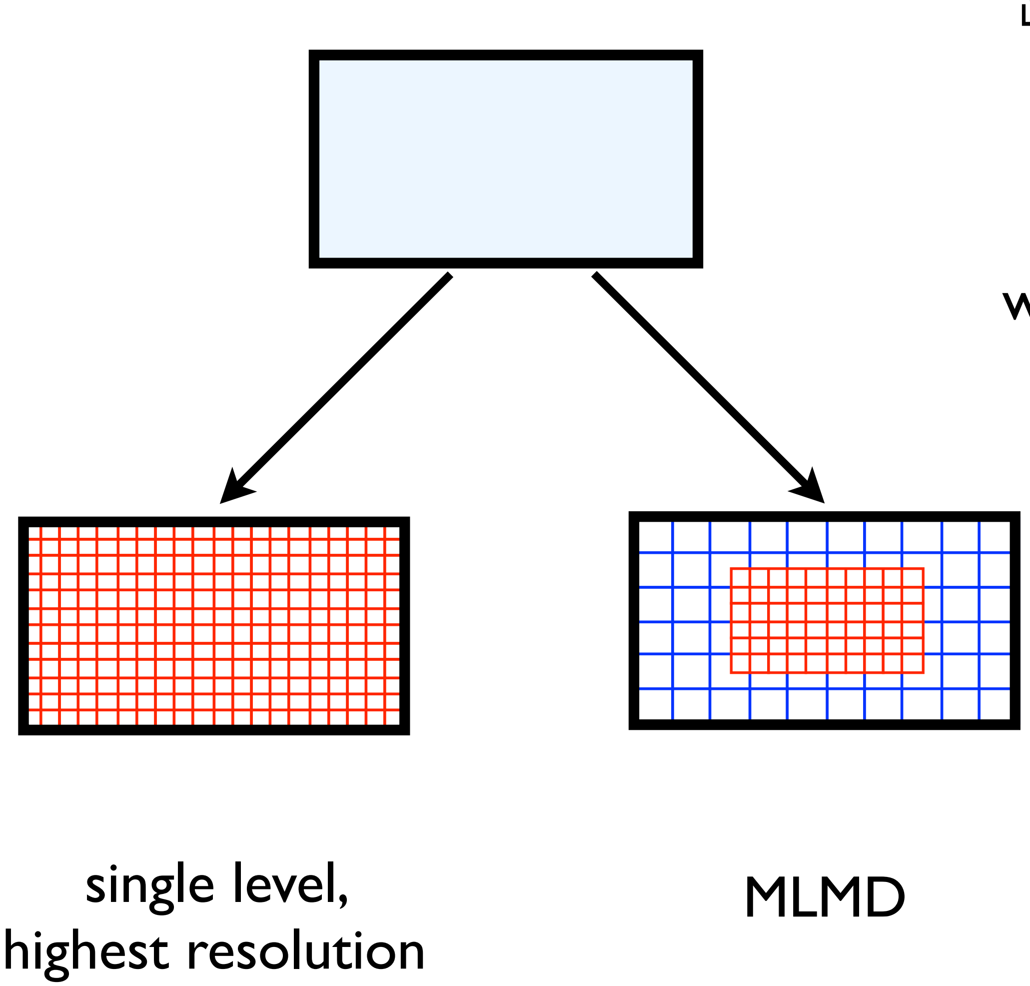

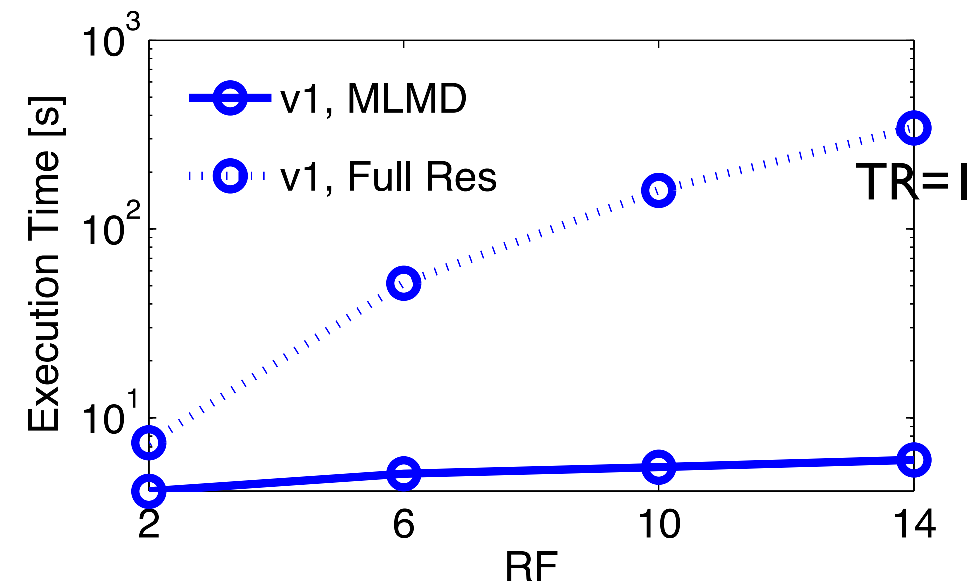

Computing resources are massively saved with respect to single level simulations

but this is a lower boundary, further speed-up can be achieved with higher Time Ratios and, more importantly, with better code architecture

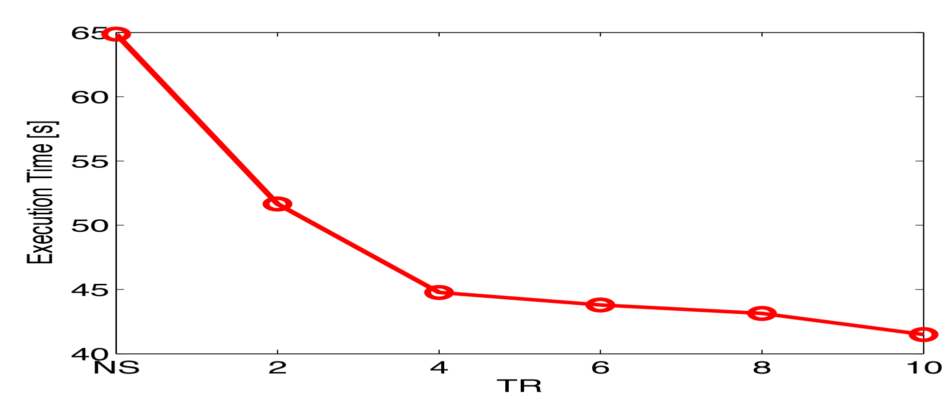

P2: Computing resource saving

Comparing the computing cost of MLMD simulations with single level simulations, resolved everywhere with the highest MLMD resolution

we need this resolution only in a fraction of the domain

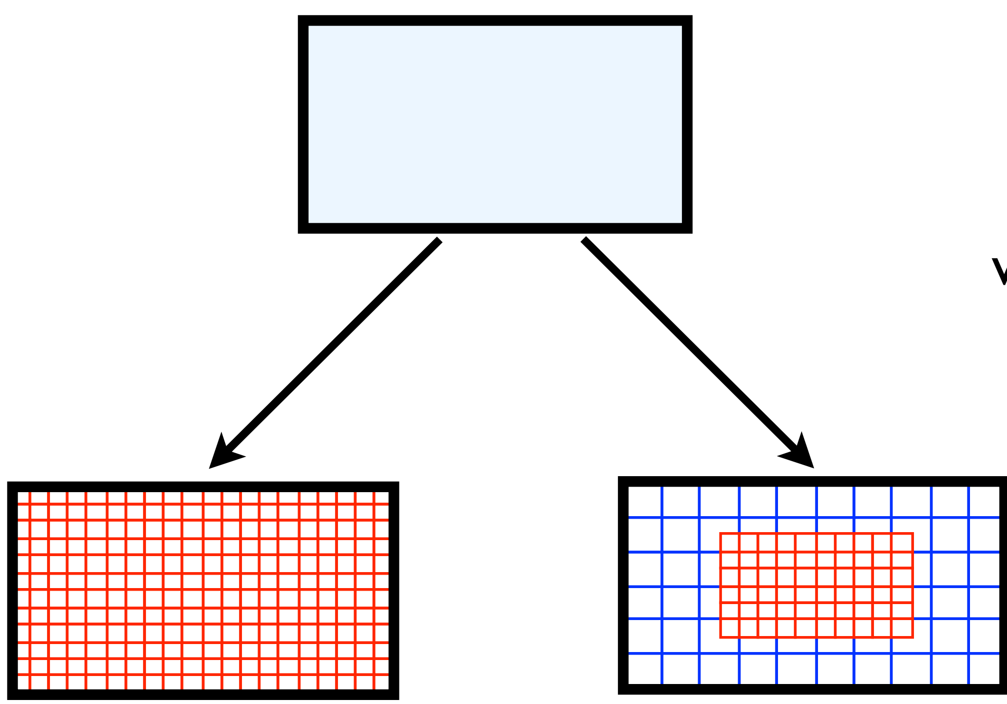

single level, highest resolution

MLMD

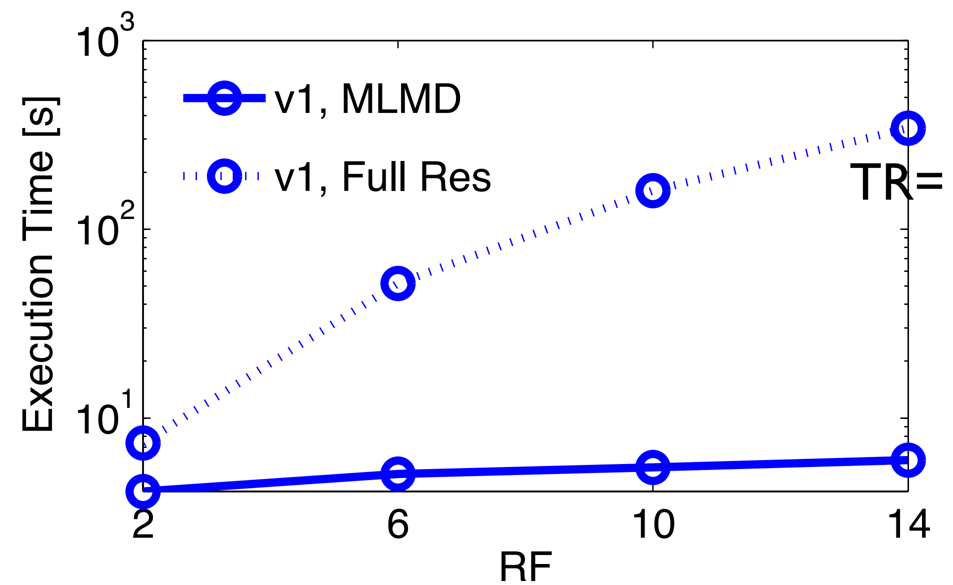

Computing resources are massively saved with respect to single level simulations

but this is a lower boundary, further speed-up can be achieved with higher Time Ratios and, more importantly, with better code architecture

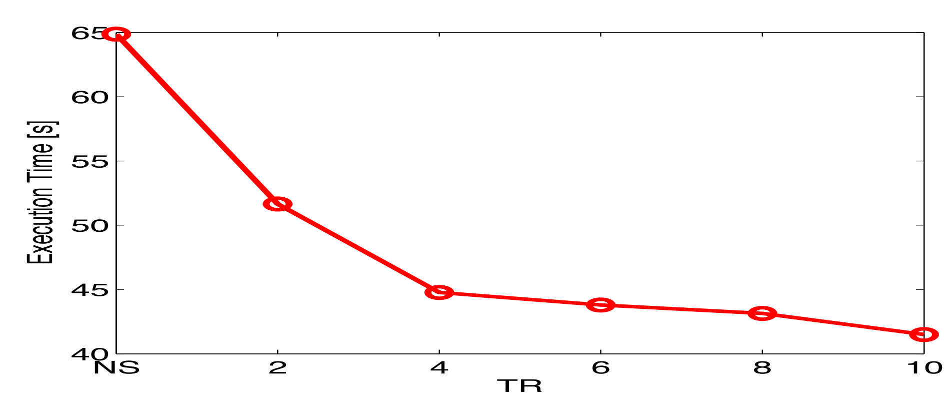

→ notable computating resources saved for "suitable" problems i.e. when it makes physical sense to use higher resolution only in a smaller fraction of the entire domain

P3: Collisionless magnetic reconnection: the essential facts

Magnetic reconnection is a change in the magnetic field line connectivity associated to *fast* energy release → stored magnetic field energy is converted into kinetic energy and heat

Magnetic reconnection is a key process in astrophysical and space plasmas
→ e.g. Sun-Earth connection and space weather

Sweet-Parker vs Petschek vs fast kinetic reconnection

under which conditions does reconnection happen?

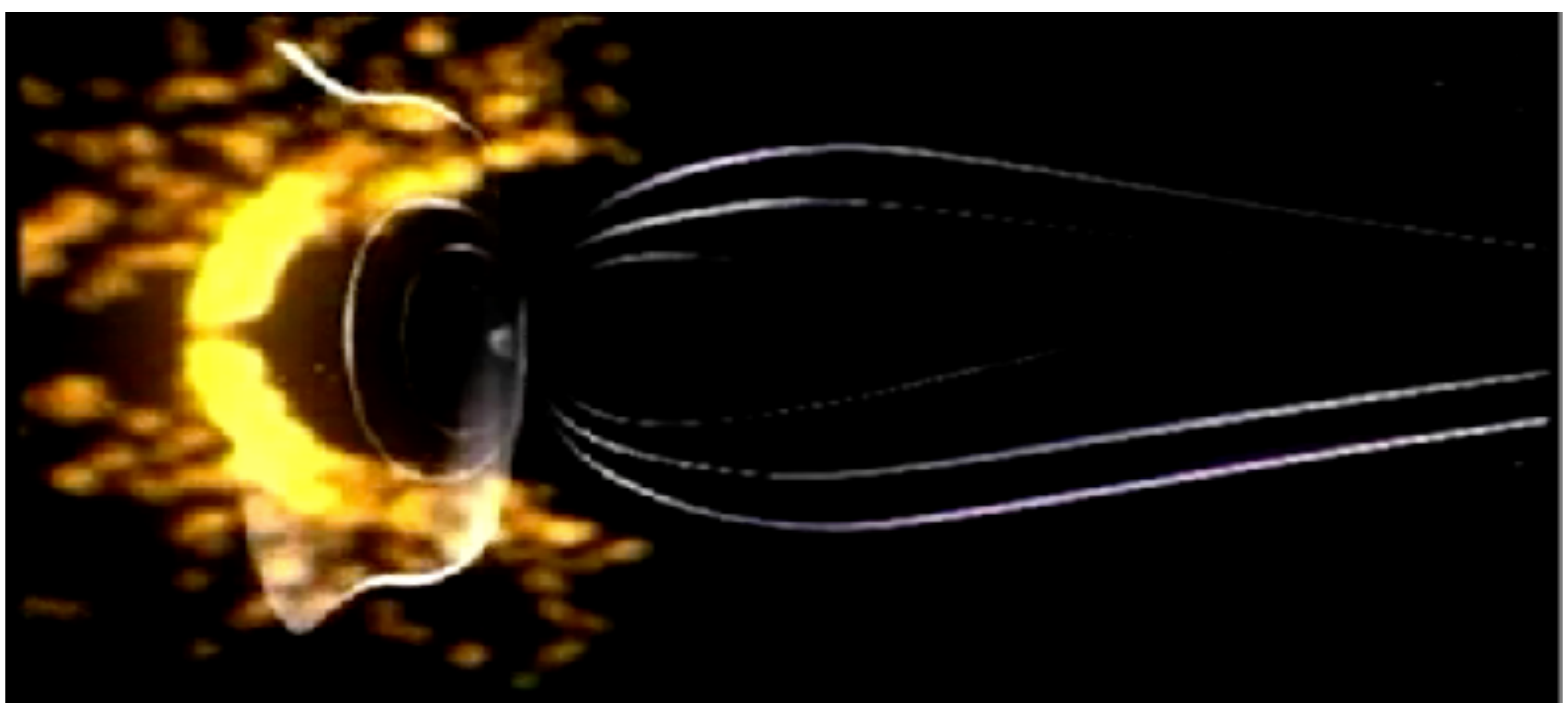

the Sun-Earth connection and the open magnetosphere
Credits: NASA

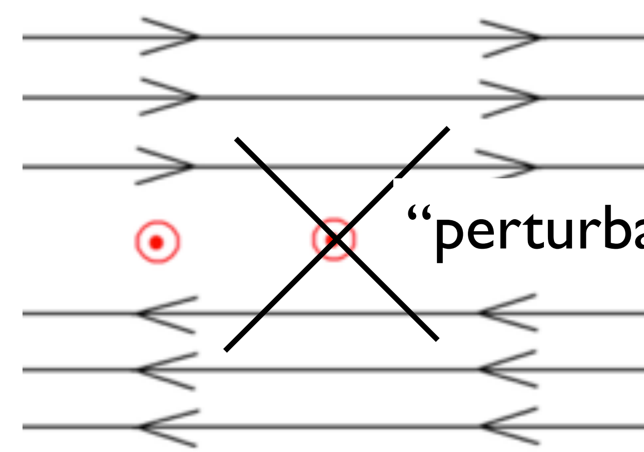

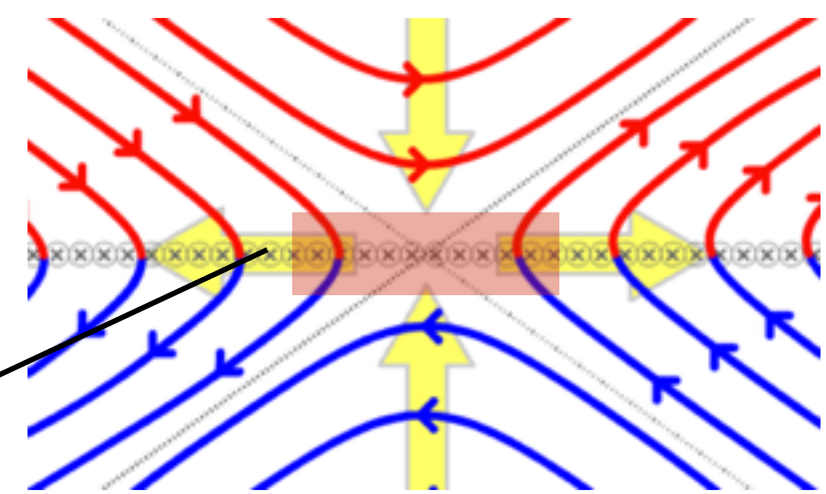

“non ideal” effects break magnetic field lines

P3: Collisionless magnetic reconnection: the essential facts

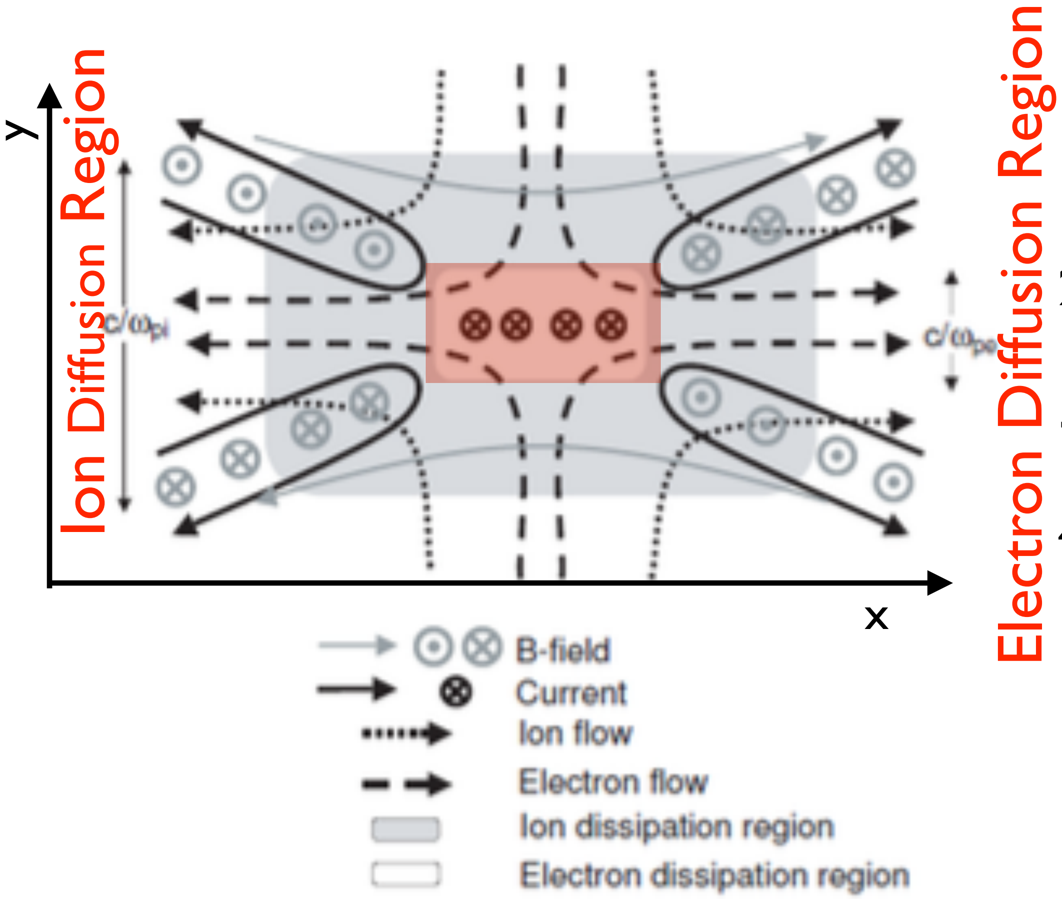

in collisionless magnetic reconnection (without guide field), fast reconnection is given by species separation - Hall term:

1. ions decouple first (heavier)
2. electrons decouple last → species separation, Electron and Ion Diffusion Regions*
3. in- plane currents lead to out of plane magnetic field Bz → characteristic quadrupolar structure*
4. in- plane electric field is given by Hall term in generalized Ohm's law*

$$\mathbf{E} = -\mathbf{v_i} \times \mathbf{B} + \frac{1}{en_e}(\mathbf{J} \times \mathbf{B} - \nabla \cdot \mathbf{P}_e) - \frac{m_e}{e}\frac{d\mathbf{v_e}}{dt}$$

ideal term | Hall term | pressure term | inertia term

* *verify during Hands on*

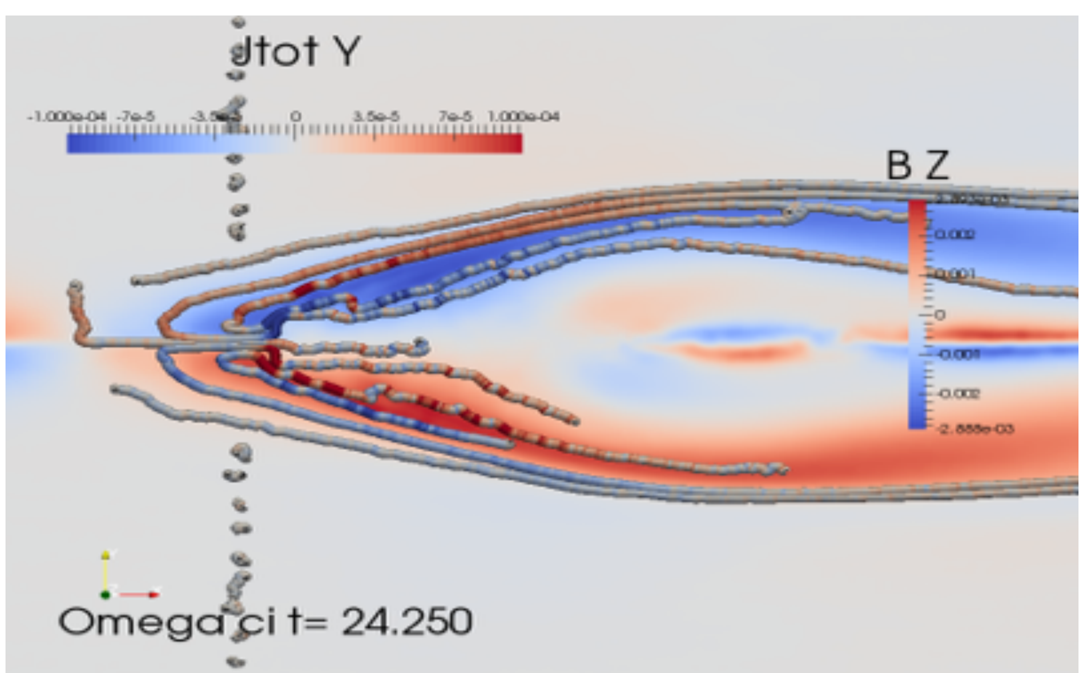

Bz, with superimposed current stream lines coloured with Jtot,y

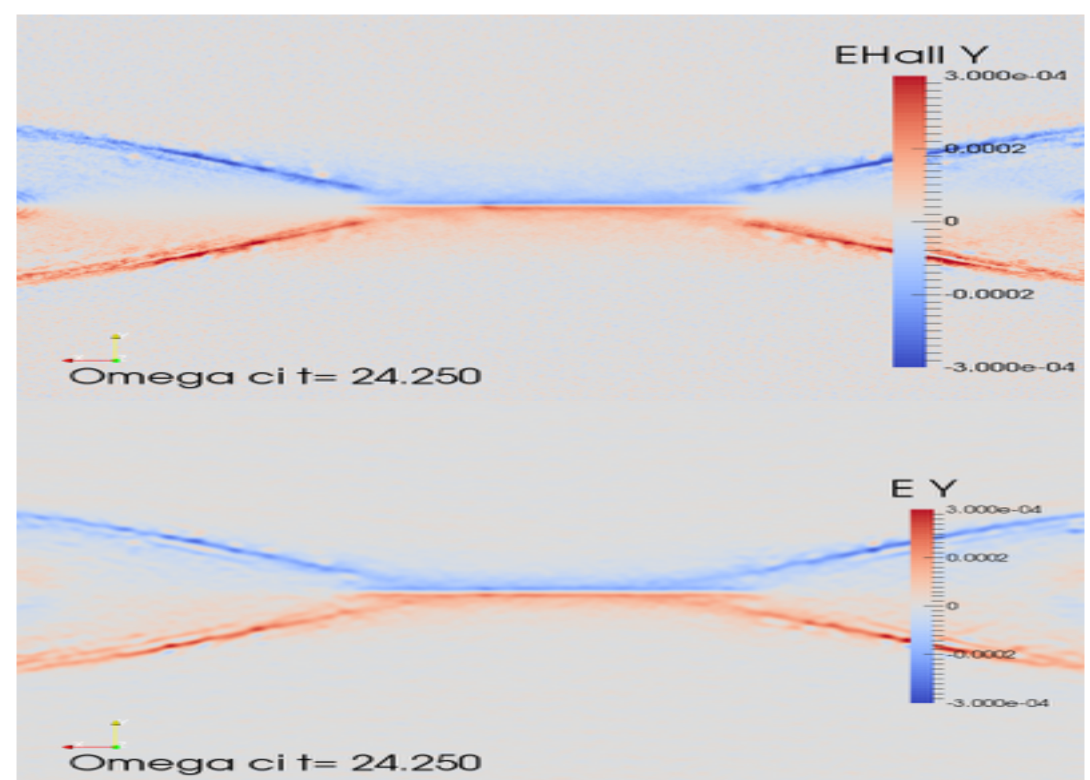

Birn 2001, 2007

P3: Energetically relevant regions in magnetic reconnection

The J.E metric [Goldman15] highlights the areas where the electric field does work on particles in magnetic reconnection → areas relevant under the energetic point of view*

** verify during Hands on*

Separatrices

Dipolarization fronts

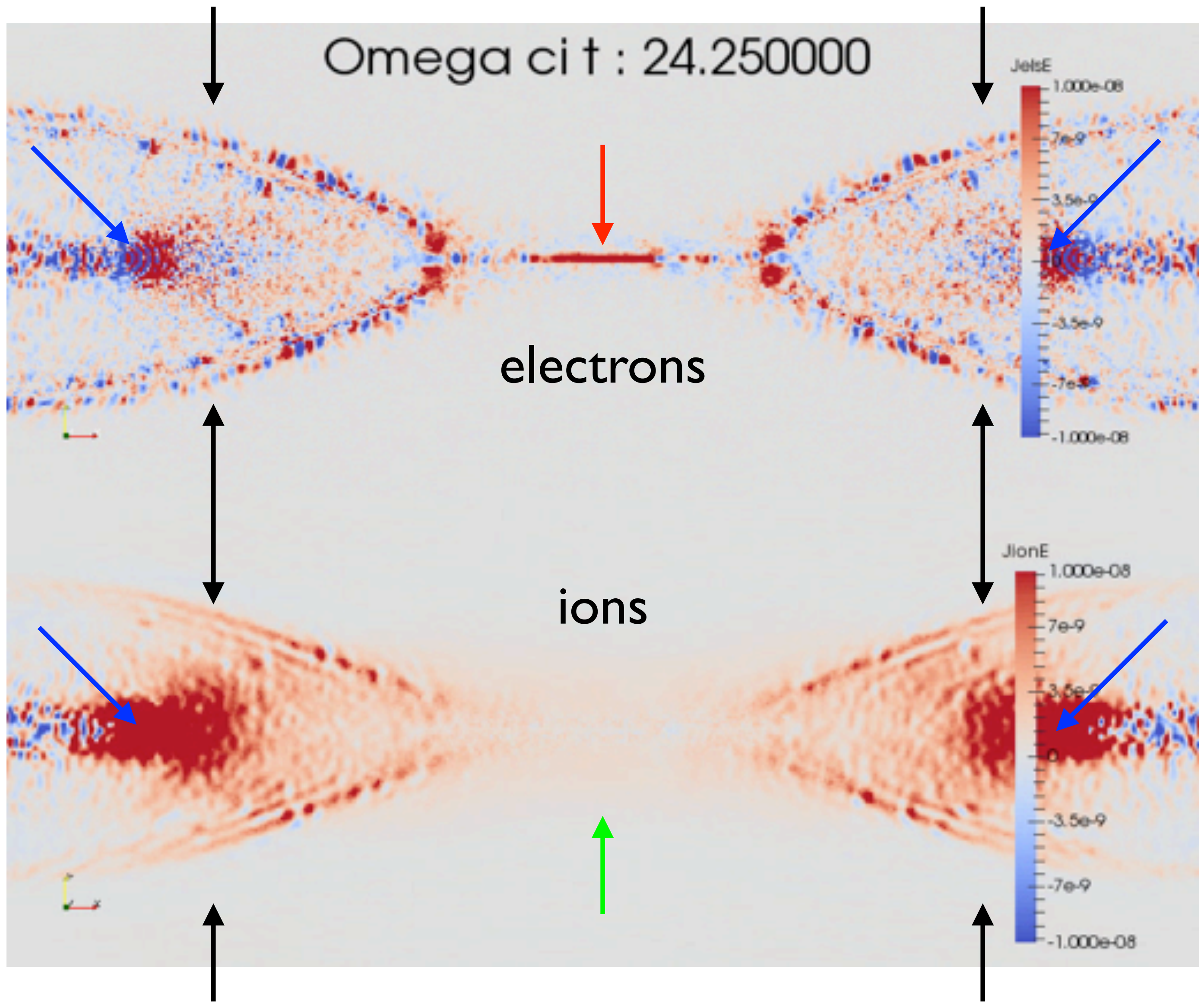

Electron Diffusion Region (EDR)

Ion Diffusion Region (IDR)

$\Delta_{IDR} \sim d_i$ (ion skin depth) ; $\Delta_{EDR} \sim d_e$ (electron skin depth)*; $d_i / d_e = \sqrt{(m_i/m_e)}$

Also, in IDR electrons are still magnetised → processes of interest at the ion scale

in EDR, electrons are unmagnetised too → processes of interest at the electron scale

→ MLMD to retain the significant physical processes in the different regions, at a very low computational cost

P3: Energetically relevant regions in magnetic reconnection

The J.E metric [Goldman15] highlights the areas where the electric field does work on particles in magnetic reconnection → areas relevant under the energetic point of view*

** verify during Hands on*

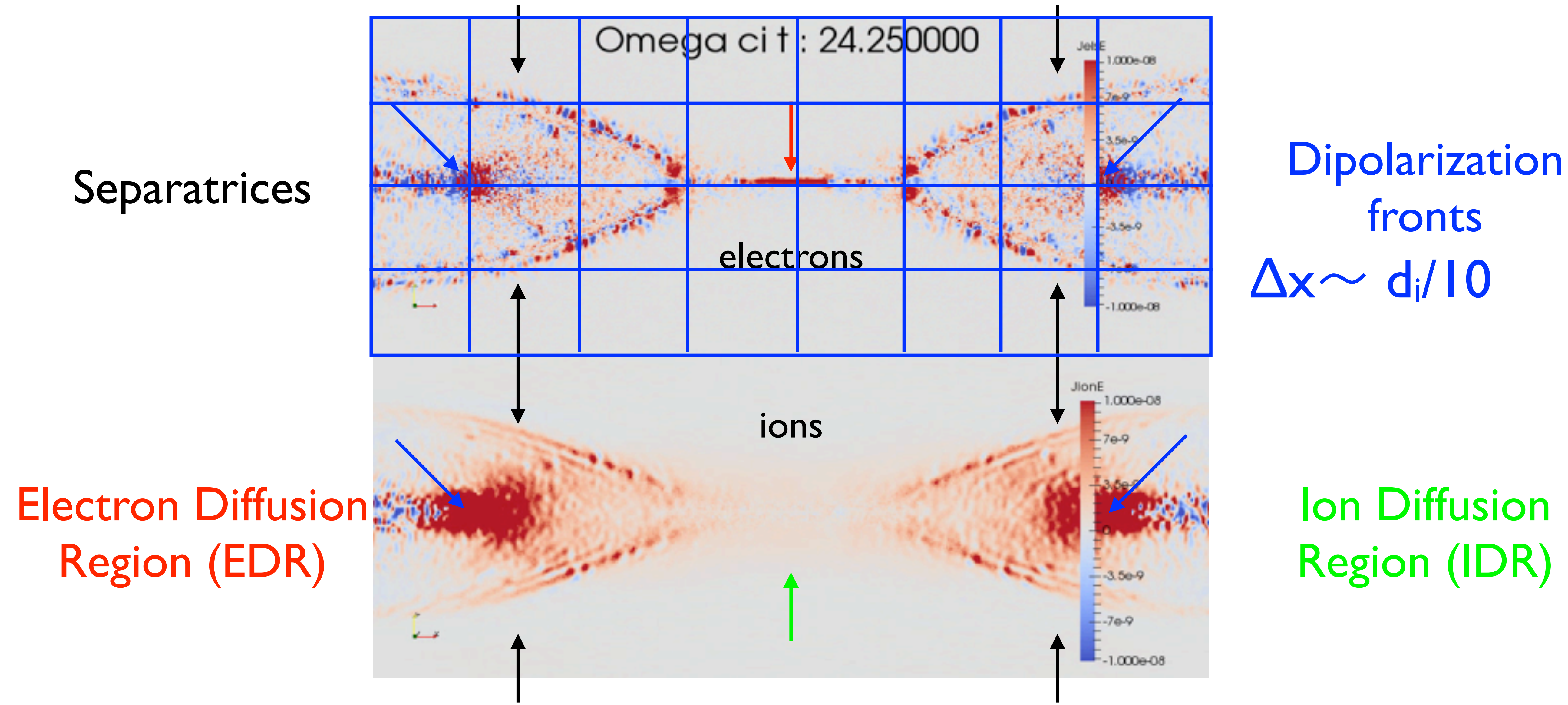

$\Delta_{IDR} \sim d_i$ (ion skin depth) ; $\Delta_{EDR} \sim d_e$ (electron skin depth)*; $d_i / d_e = \sqrt{(m_i/m_e)}$

Also, in IDR electrons are still magnetised → processes of interest at the ion scale

in EDR, electrons are unmagnetised too → processes of interest at the electron scale

→ MLMD to retain the significant physical processes in the different regions, at a very low computational cost

P3: Energetically relevant regions in magnetic reconnection

The J.E metric [Goldman15] highlights the areas where the electric field does work on particles in magnetic reconnection → areas relevant under the energetic point of view*

** verify during Hands on*

Separatrices

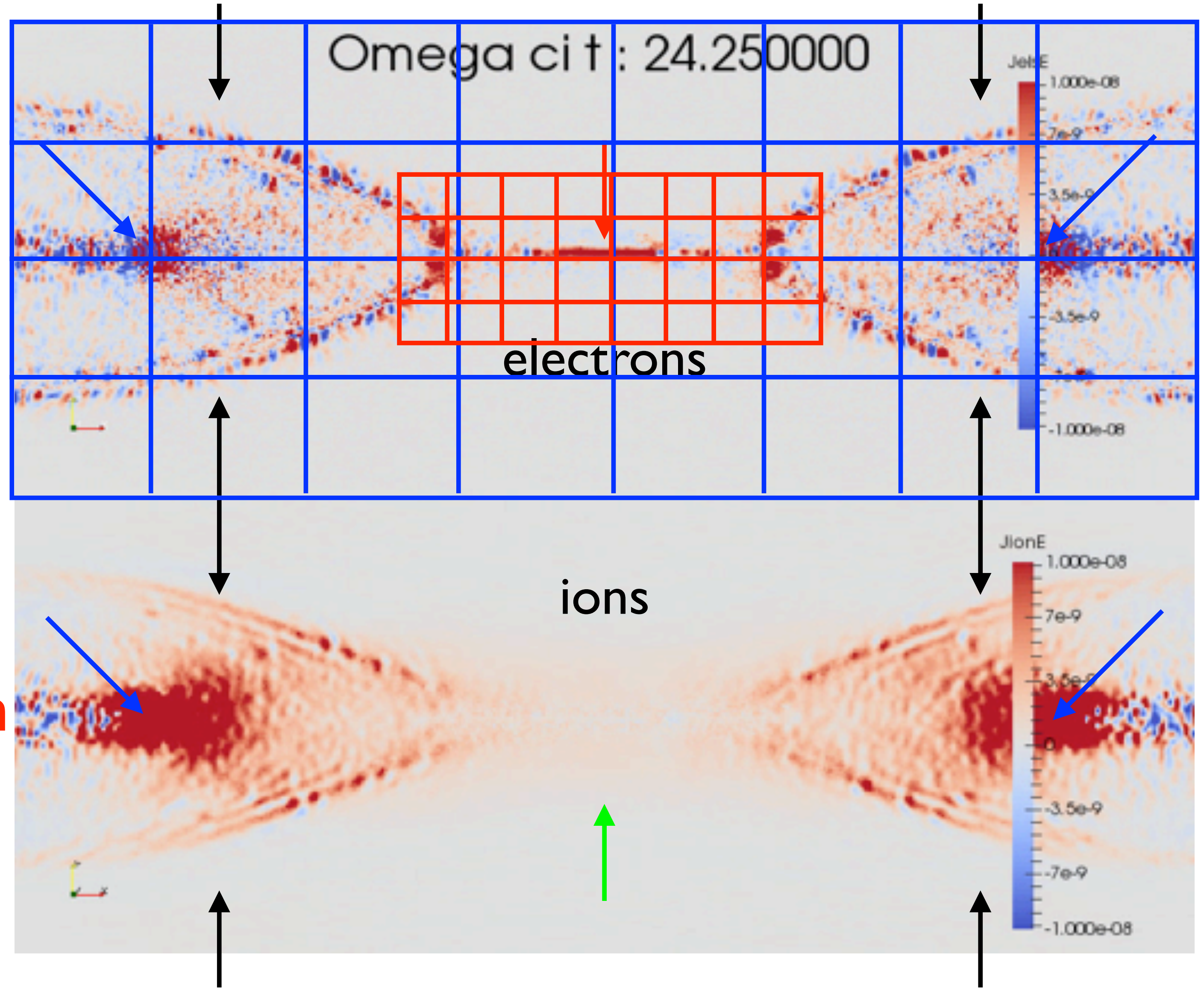

Dipolarization fronts

$\Delta x \sim d_i/10$

$\Delta x \sim d_e/10$

Electron Diffusion Region (EDR)

Ion Diffusion Region (IDR)

$\Delta_{IDR} \sim d_i$ (ion skin depth) ; $\Delta_{EDR} \sim d_e$ (electron skin depth)*; $d_i/d_e = \sqrt{(m_i/m_e)}$

Also, in IDR electrons are still magnetised → processes of interest at the ion scale

in EDR, electrons are unmagnetised too → processes of interest at the electron scale

→ MLMD to retain the significant physical processes in the different regions, at a very low computational cost

P4: MLMD simulations of magnetic reconnection

ion scale processes are resolved by both grids; electron scale processes (e.g., speed of electron jets*) are simulated by both grids but fully resolved on the refined grid only; on the coarse grid, selective damping and spectral compression are at work

$L_x = L_y = 20\ d_i = 860\ d_e$
$m_i / m_e = 1836$
RF=12
TR= 1 → 6
$dx_{CG} = 0.078\ d_i = 3.35\ d_e$
$dx_{RF} = 0.28\ d_e$
$dt_{CG} = 0.05 \rightarrow 0.3 \omega_{pi}^{-1}$
$dt_{RF} = 0.05\ \omega_{pi}^{-1}$

very cheap realistic mass ratio simulations!!!

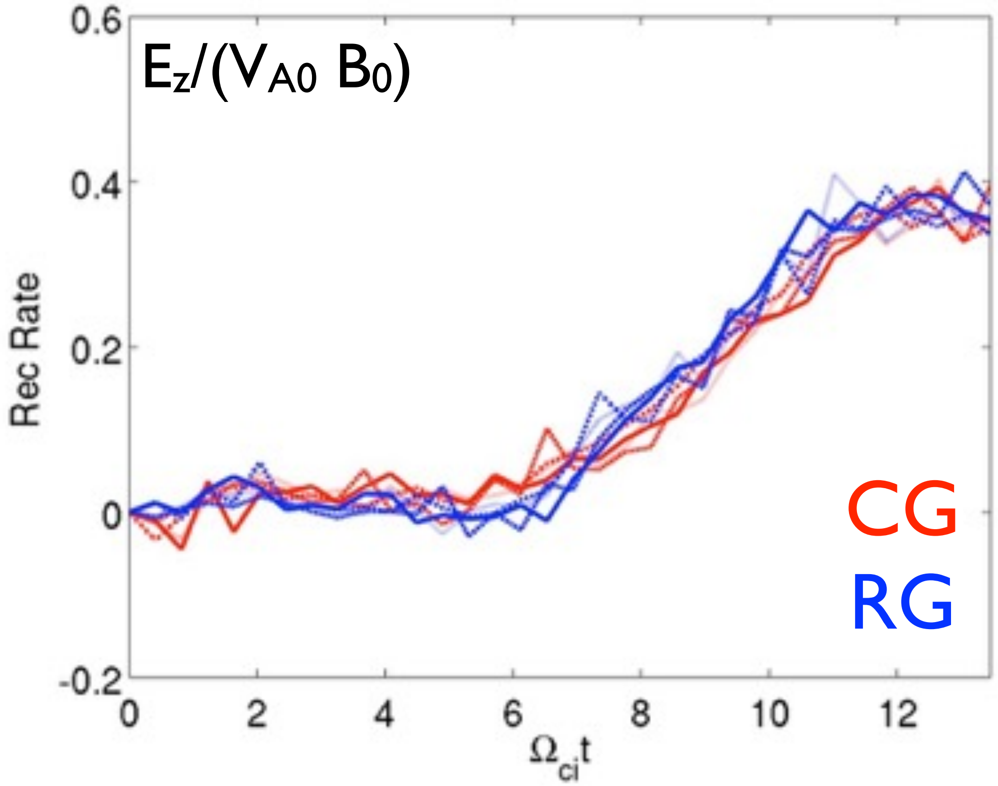

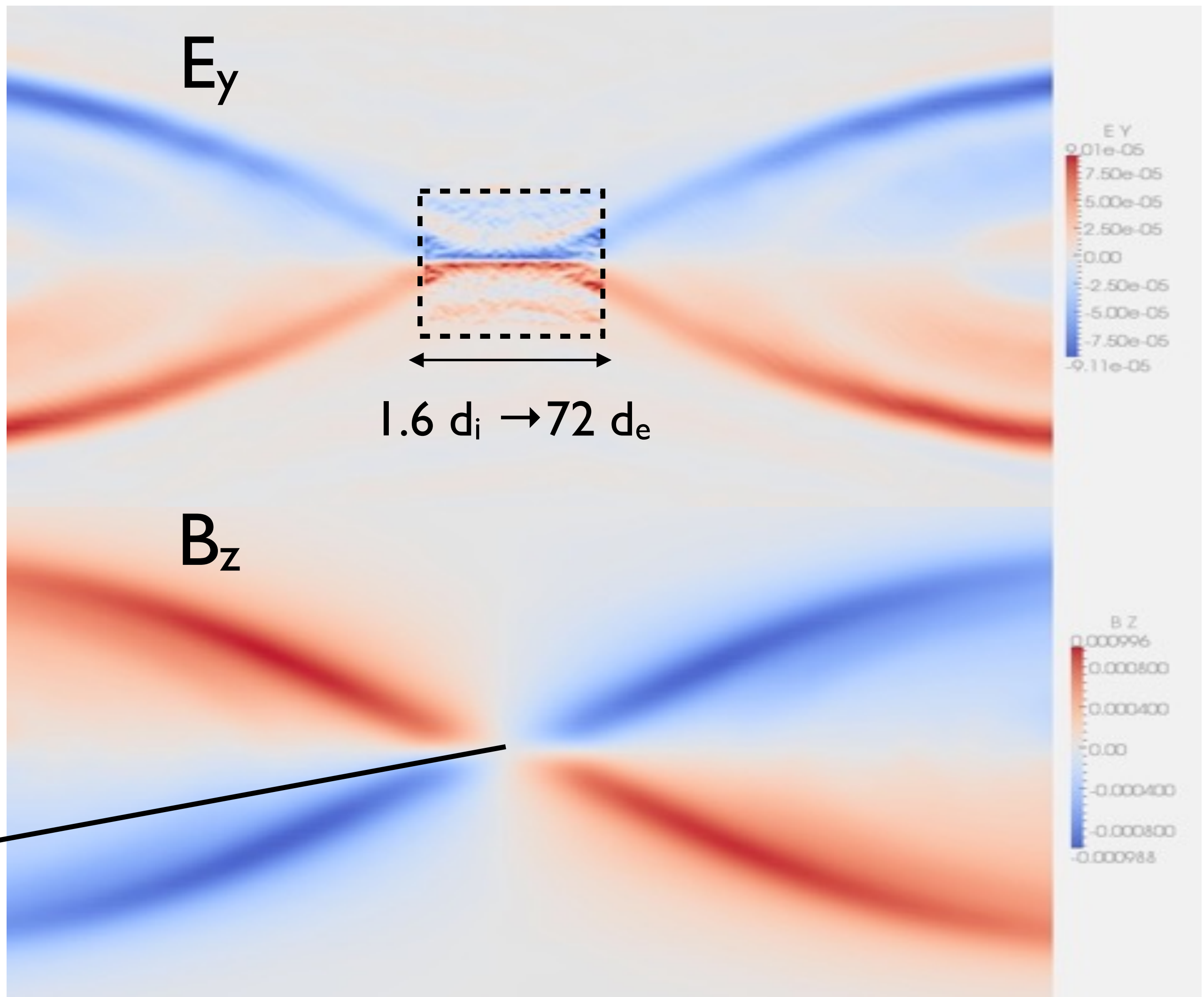

large scale processes reproduced by both grids: reconnection rate, Harris field, quadrupolar Bz structure

P4: MLMD simulations of magnetic reconnection

ion scale processes are resolved by both grids; electron scale processes (e.g., speed of electron jets*) are simulated by both grids but fully resolved on the refined grid only; on the coarse grid, selective damping and spectral compression are at work

Electron scale processes are reproduced by the refined grid
e.g.: formation of jets at the X point with velocity $v_{A,e}$

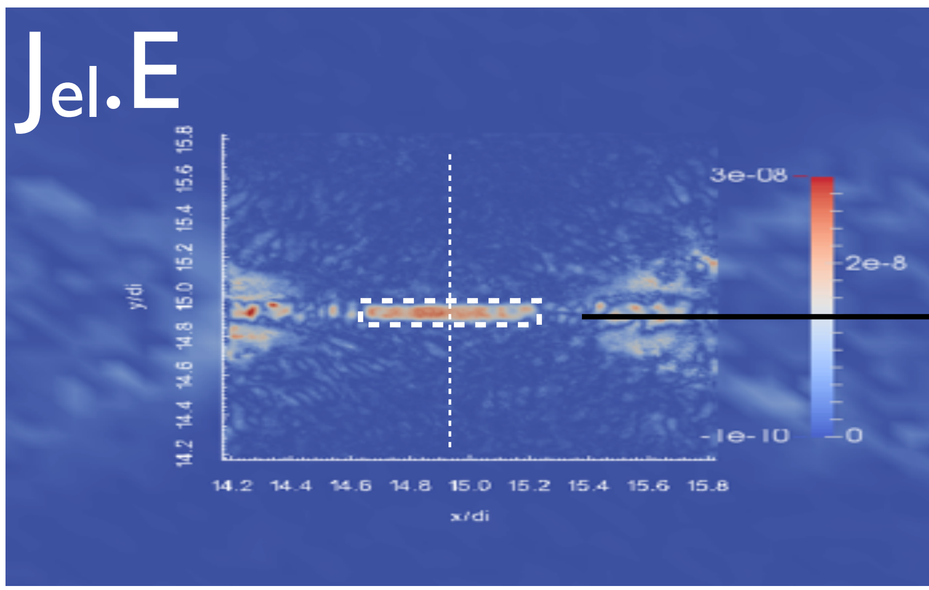

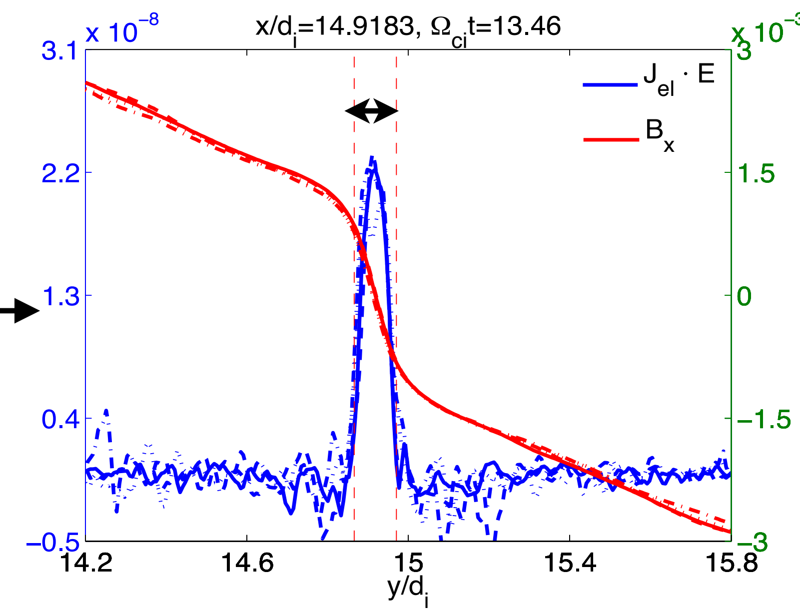

calculation of the ion Alfven speed: identification of the Electron Diffusion Region with the J.E method

The $B_{x,up}$ used in the calculation of the Alfven speed

$$v_{A,i} = B_{x,up}/\sqrt{\mu_0 m_i n_i}$$

is obtained averaging the B_x values on the upper and lower EDR boundaries

$|v_{e,x}/v_{A,i}|$

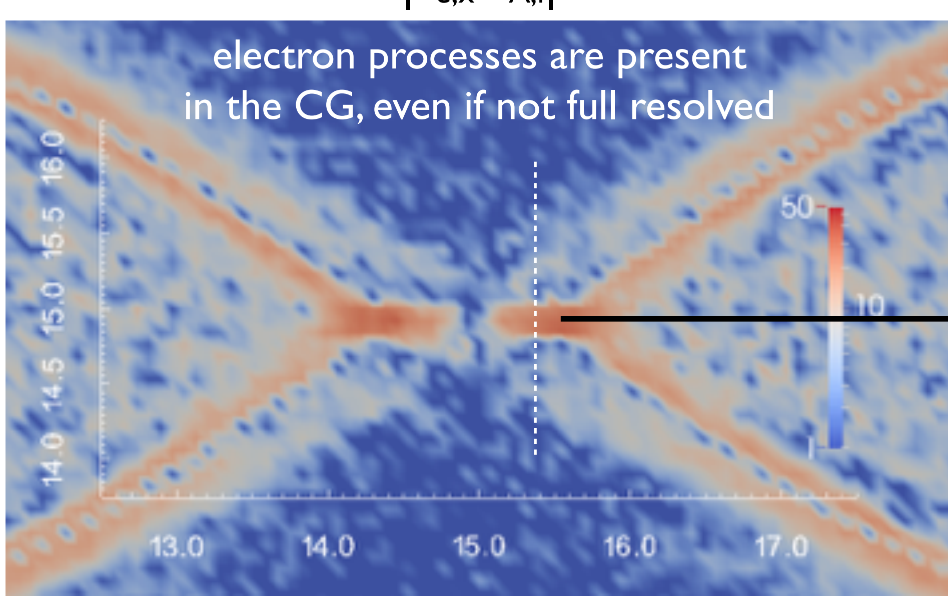

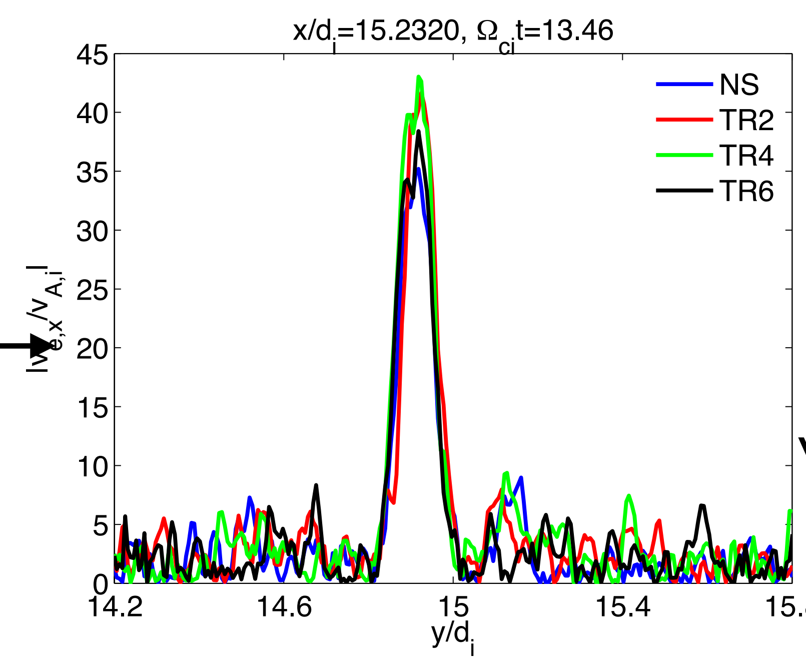

electron jet velocity, normalized to the ion Alfven

as expected from Drake08,
$v_{e,x}/v_{A,i} = v_{A,e}/v_{A,i} \sim \sqrt{(m_i/m_e)} \sim 43$

P4: MLMD simulations of magnetic reconnection

ion scale processes are resolved by both grids; electron scale processes (e.g., speed of electron jets*) are simulated by both grids but fully resolved on the refined grid only; on the coarse grid, selective damping and spectral compression are at work

Electron scale processes are reproduced by the refined grid
e.g.: formation of jets at the X point with velocity $v_{A,e}$

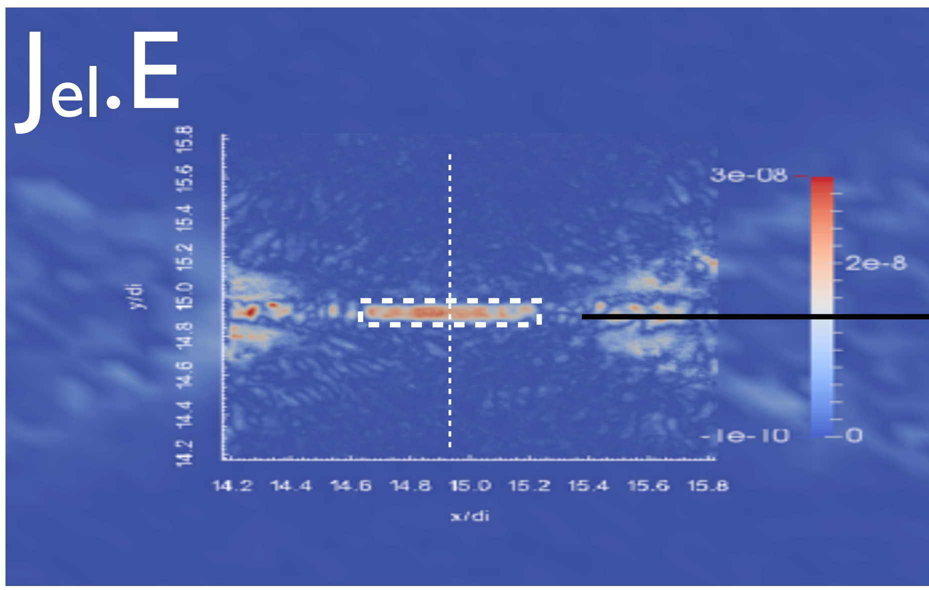

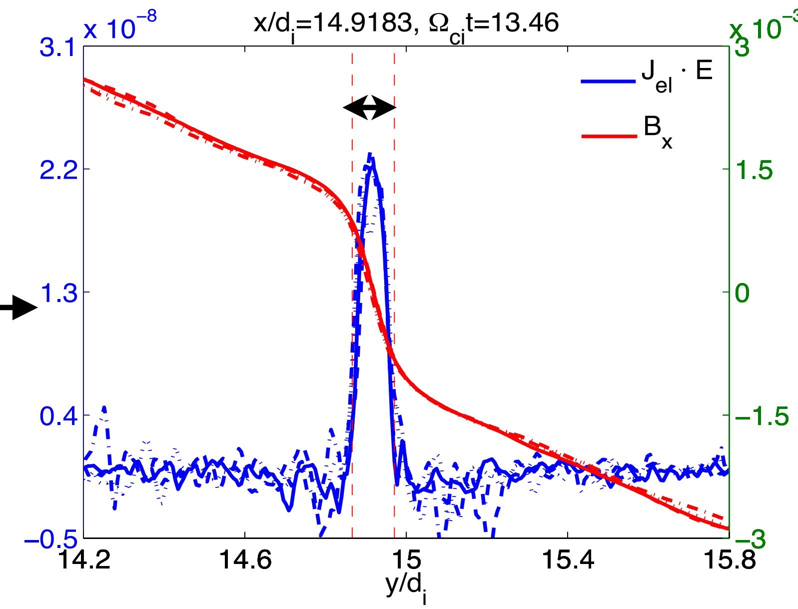

calculation of the ion Alfven speed: identification of the Electron Diffusion Region with the J.E method

The $B_{x,up}$ used in the calculation of the Alfven speed

$$v_{A,i} = B_{x,up}/\sqrt{\mu_0 m_i n_i}$$

is obtained averaging the B_x values on the upper and lower EDR boundaries

$|v_{e,x}/v_{A,i}|$

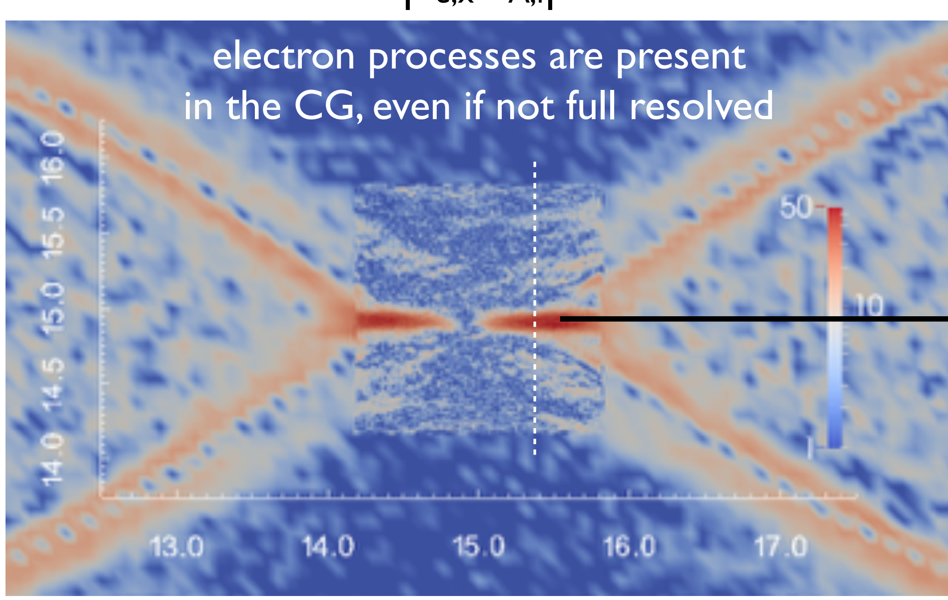

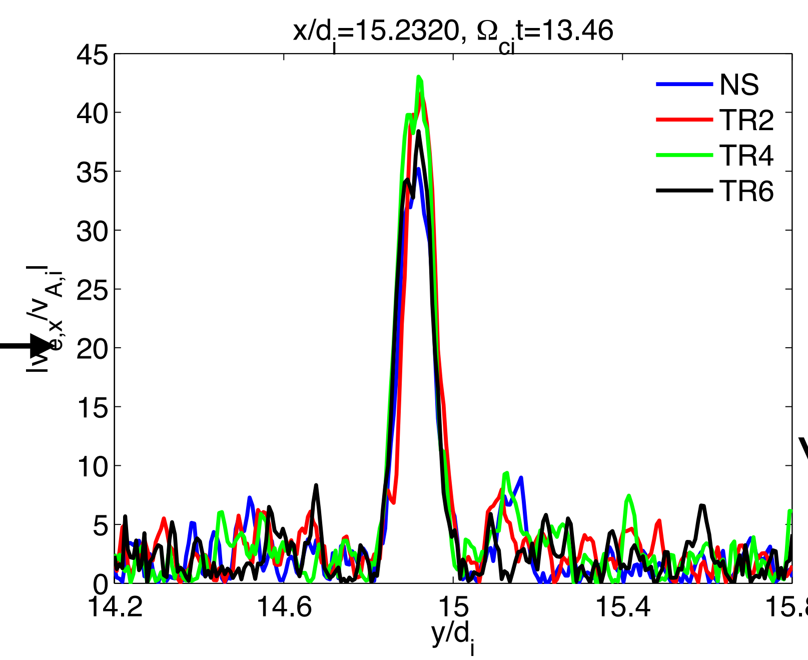

electron jet velocity, normalized to the ion Alfven

as expected from Drake08,
$v_{e,x}/v_{A,i} = v_{A,e}/v_{A,i} \sim \sqrt{(m_i/m_e)} \sim 43$

P5: MLMD simulations of turbulence generated by the Lower Hybrid Drift Instability (LHDI)

Other fields of application of the MLMD method: cases when multiple scales coexist self-similarly in a large domain

→ a representative part of the large domain is simulated with higher resolution

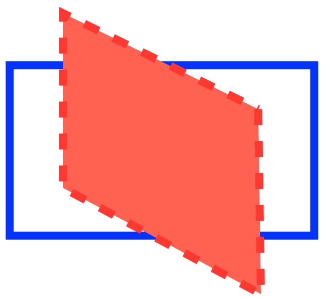

e.g.: simulations of Lower Hybrid Drift Instability.

The LHDI:

1) is driven by a density gradient in presence of a perpendicular field

2) is unstable over a large range of wavenumber and frequencies;

fast branch with $\gamma \sim \Omega_{LH}$, $k \sim 1/\rho_e$, ES, slow branch at $k \sim 1/\sqrt{(\rho_e \rho_i)}$, EM

3) breaks large scale fields in smaller and smaller structures → acts as a "turbulence generator"

electron density | B_z field component

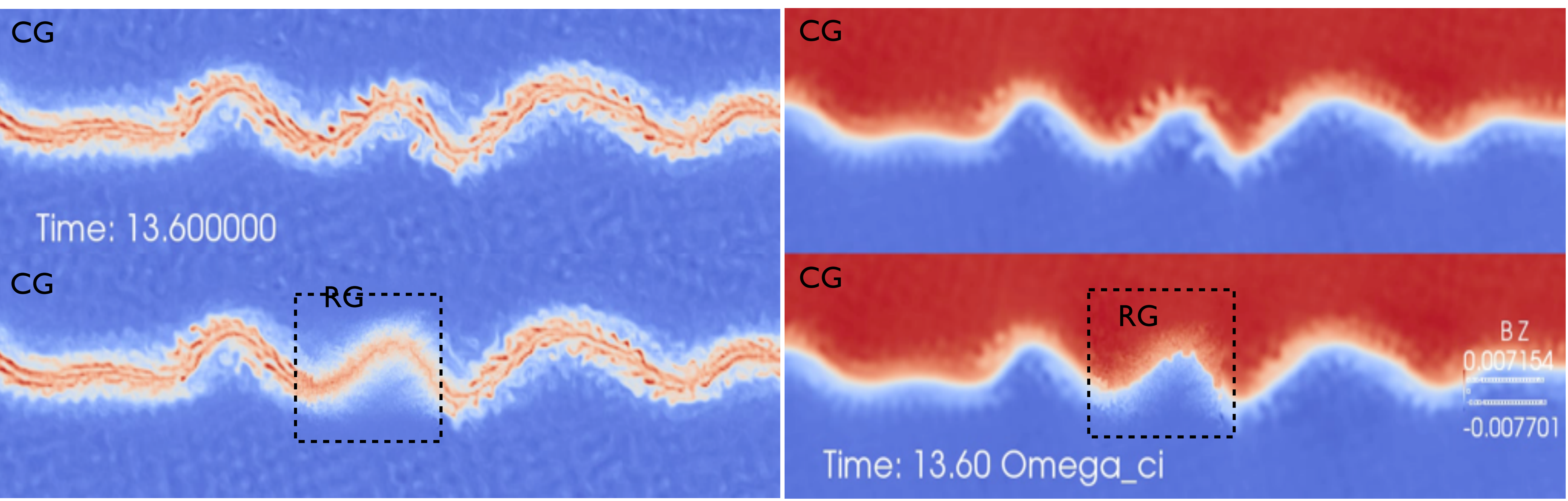

the refined grid is driven by the coarse grid in the low wavenumber range; the refined grid cascades to the small scales which the coarse grid averages out

Daughton 2003

P5: MLMD simulations of turbulence generated by the Lower Hybrid Drift Instability (LHDI)

Other fields of application of the MLMD method: cases when multiple scalea coexist self-similarly in a large domain

→ a representative part of the large domain is simulated with higher resolution

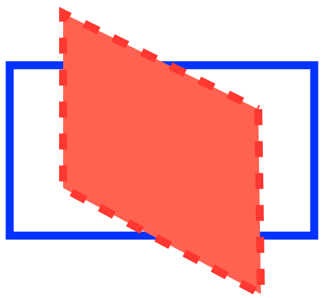

e.g.: simulations of Lower Hybrid Drift Instability.

The LHDI:

1) is driven by a density gradient in presence of a perpendicular field

2) is unstable over a large range of wavenumber and frequencies;

fast branch with $\gamma \sim \Omega_{LH}$, $k \sim 1/\rho_e$, ES, slow branch at $k \sim 1/\sqrt{(\rho_e \rho_i)} \sim 20$, EM

3) breaks large scale fields in smaller and smaller structures → acts as a "turbulence generator"

electron density | B_z field component

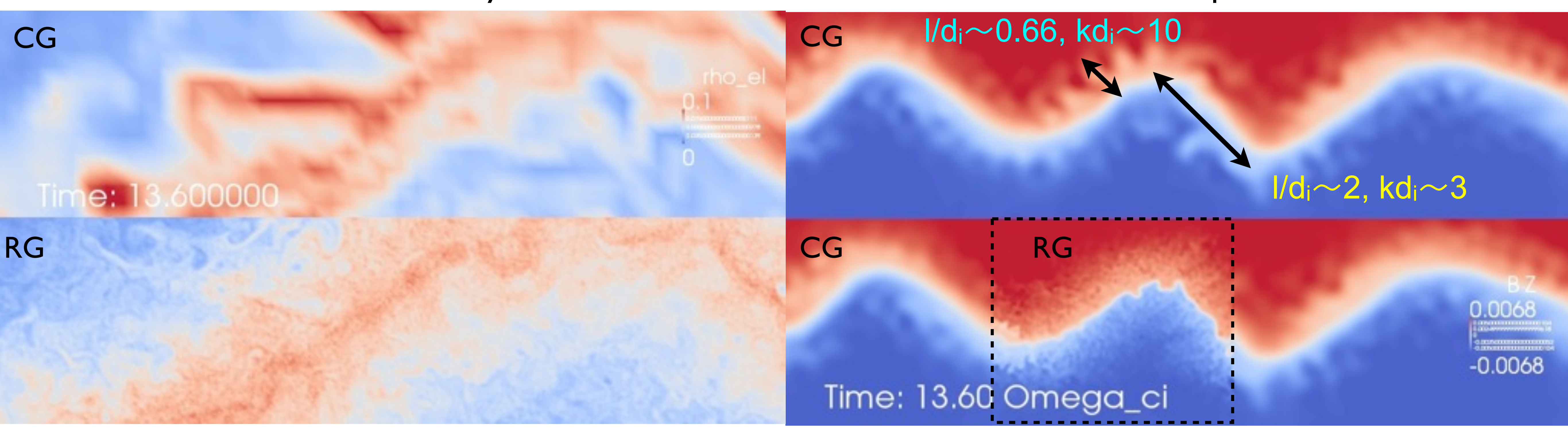

the refined grid is driven by the coarse grid in the low wavenumber range; the refined grid cascades to the small scales which the coarse grid averages out

Daughton 2003

P5: simulations of turbulence: challenges and MLMD solutions

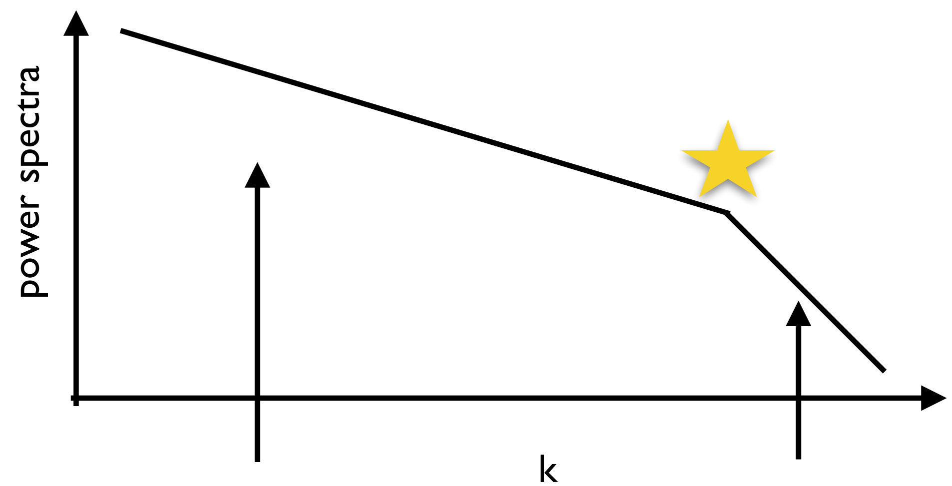

In turbulent environment, energy is transported from the large to the small scales over several wavenumber decades (inertial range); the turbulent cascade is often broken by wave- particle interaction processes

e.g.: candidate for the solar wind: interaction of protons with kinetic Alfven wave, proton cyclotron damping, electron or ion Landau damping

large scales of energy injection

small scales of energy dissipation

→ high computational cost! Also, the number of particle has to be very high to reduce the numerical noise and grid effects (when using a PIC code) have to be taken into consideration

single level simulation

MLMD simulation

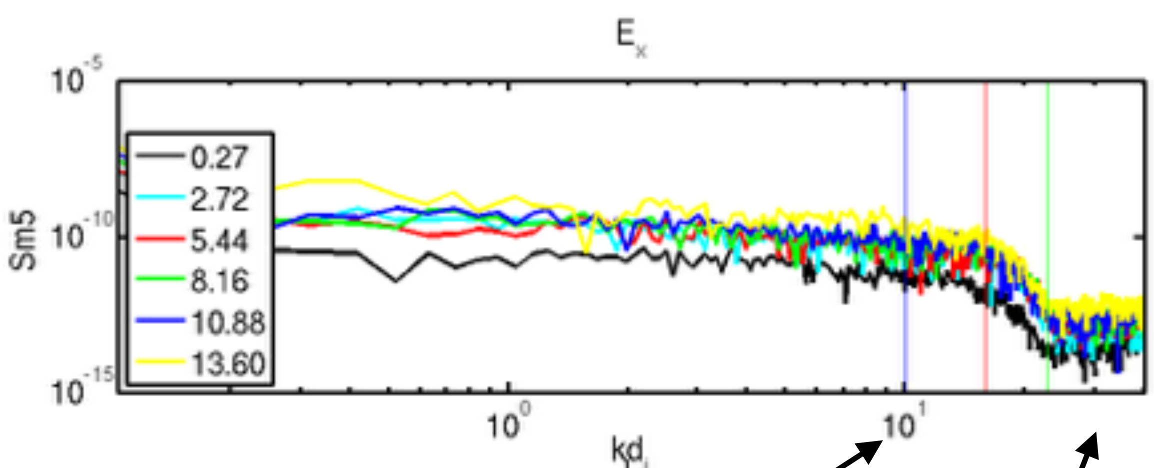

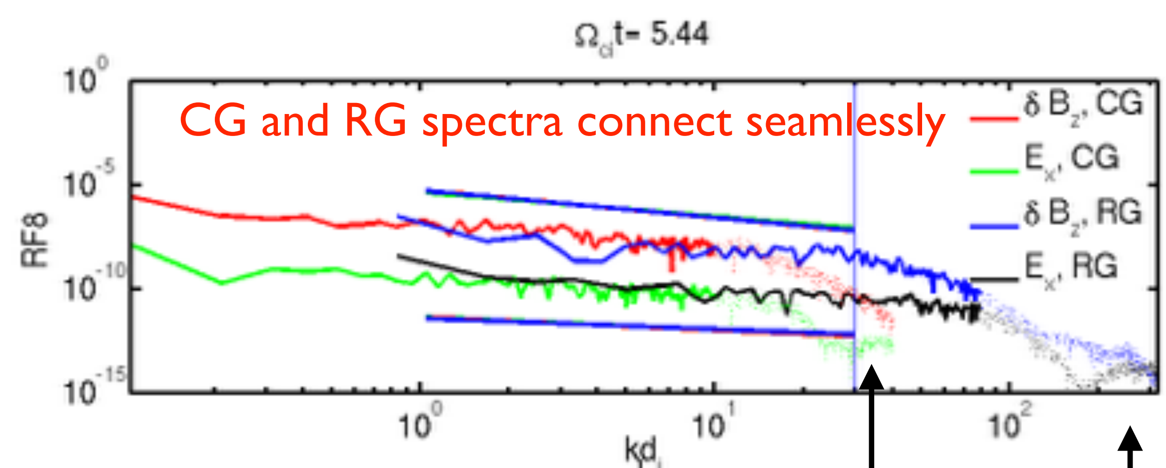

grid effects start here, $\sim k_{max}/4$

particle noise plateau

… → part of the spectra affected by grid effect and unreliable

the particle noise plateau is pushed to higher k and lower power levels (more particles per unit volume)

the RG extends the k range of a factor RF with respect to the coarse grid; the computational cost is *2 rather than $*RF^2$

P5: MLMD simulations of turbulence generated by the LHDI

Norgren 2012 observes coupling between the perpendicular electric field and magnetic field oscillations in the magnetotail in presence of LHDI waves at wavenumbers corresponding to the electrostatic LHDI branch with the perpendicular electron current as mediator. We confirm their observations and extend the study to lower wavenumber (electromagnetic LHDI branch, kink instability)

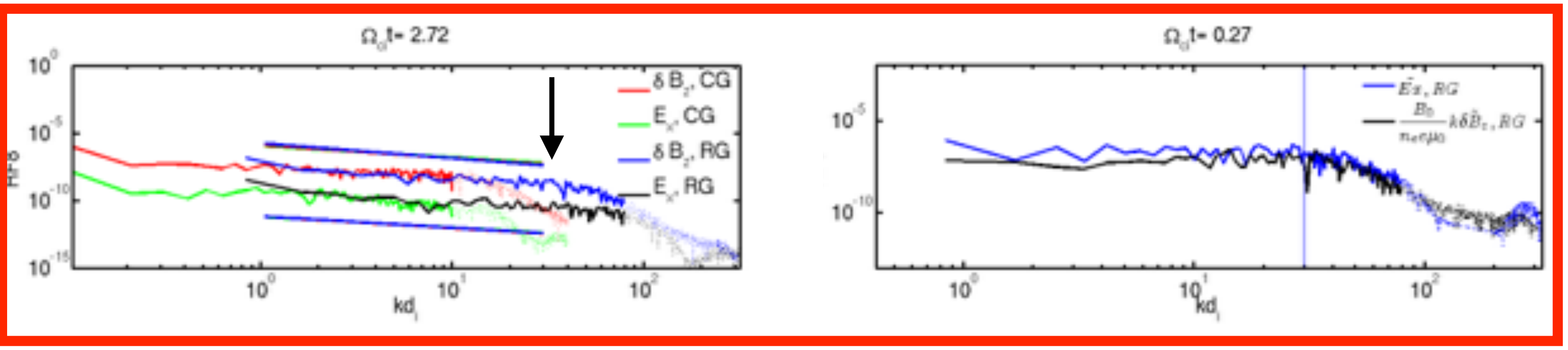

ES LHDI branch time scales and wavenumbers: Ex δBz coupling observed, electron current as mediator (Norgren12) → break in the δBz power spectra at lower, non coupled (k di ∼30) wavenumbers

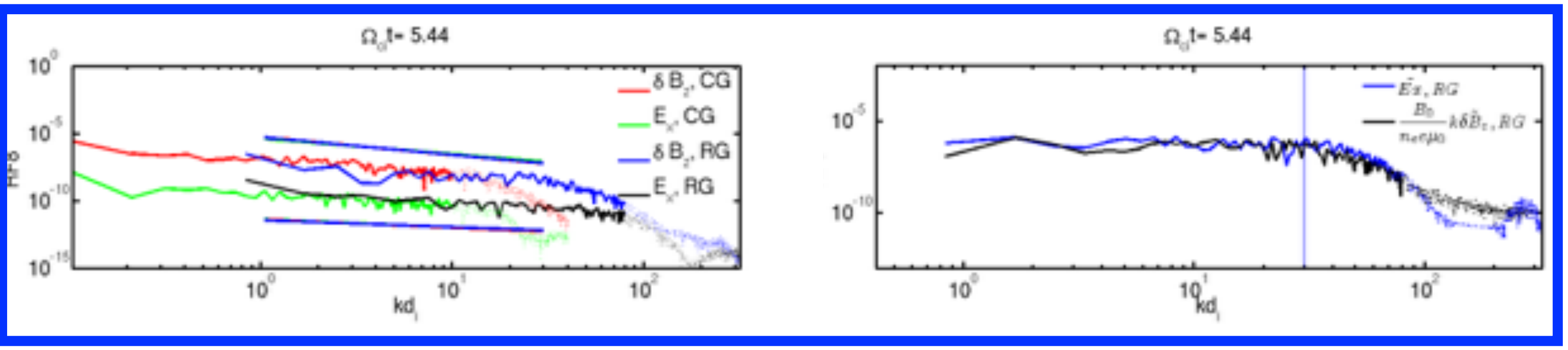

coupling extends to LHDI EM wavenumber with the onset of LHDI EM branch; mediator is still electron current, but structures at the centre of the current sheet

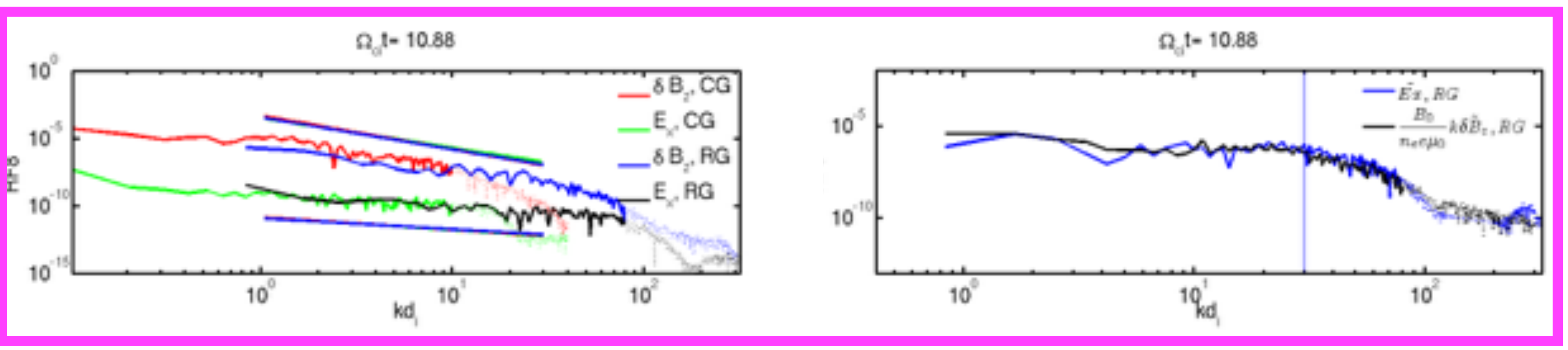

at kink mode time scales and wavenumber, background ions (Karimabadi 2003) act as mediator

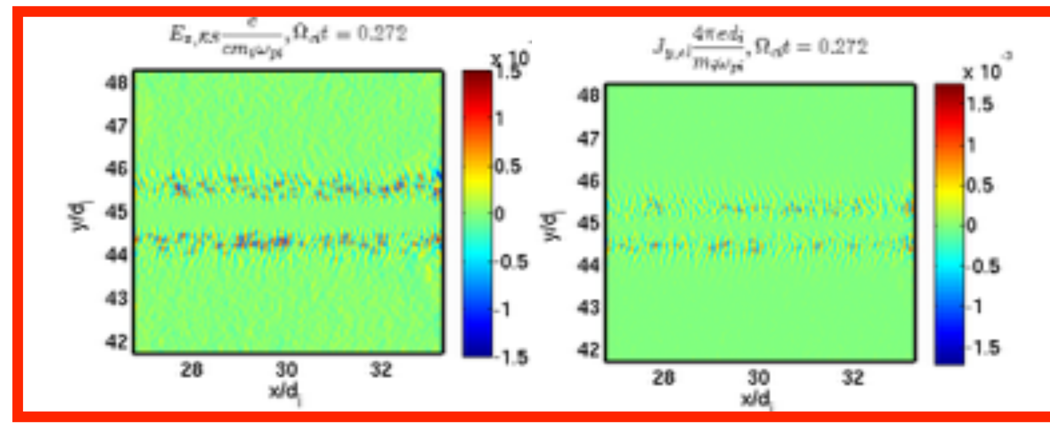

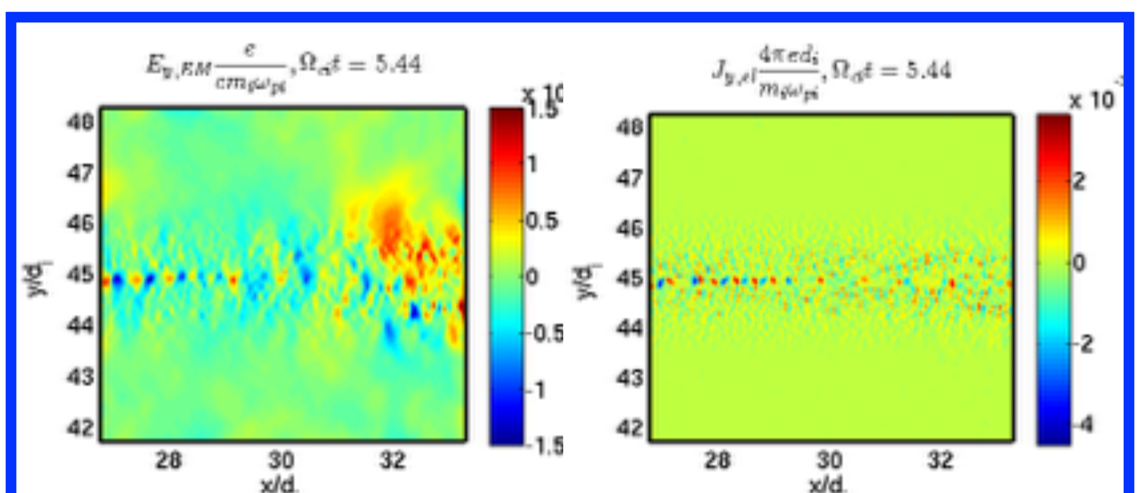

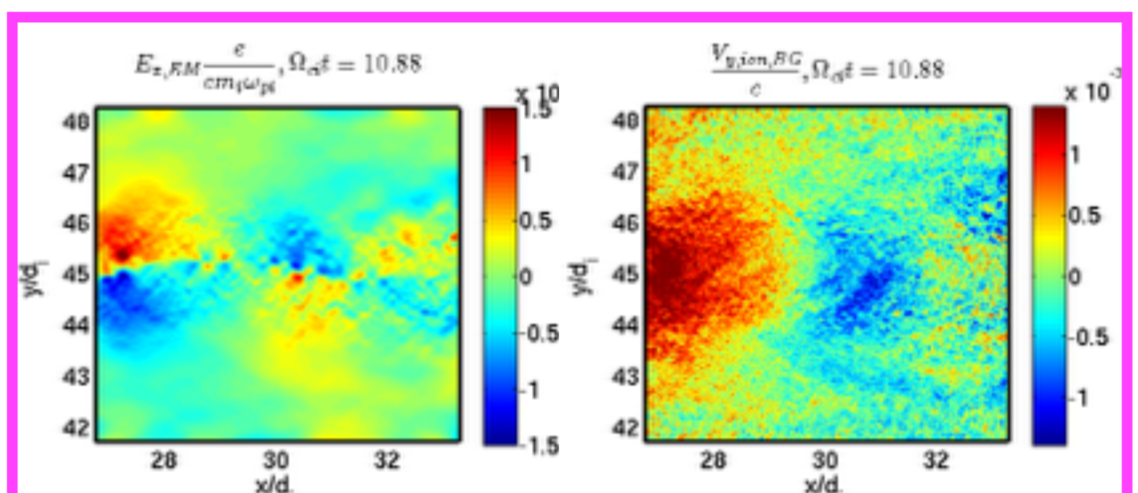

this analysis is done on the refined grid of the RF=8 MLMD simulation

Innocenti et al, in preparation

P5: Cluster observations confirming our findings

magnetotail, [-10 -3 3] RE GSM

the study done in Norgren 2012 for the fast ES LHDI branch is extended to the slow EM one

Bz, E perp coupling at both slow and fast LHDI branch as expected from our study

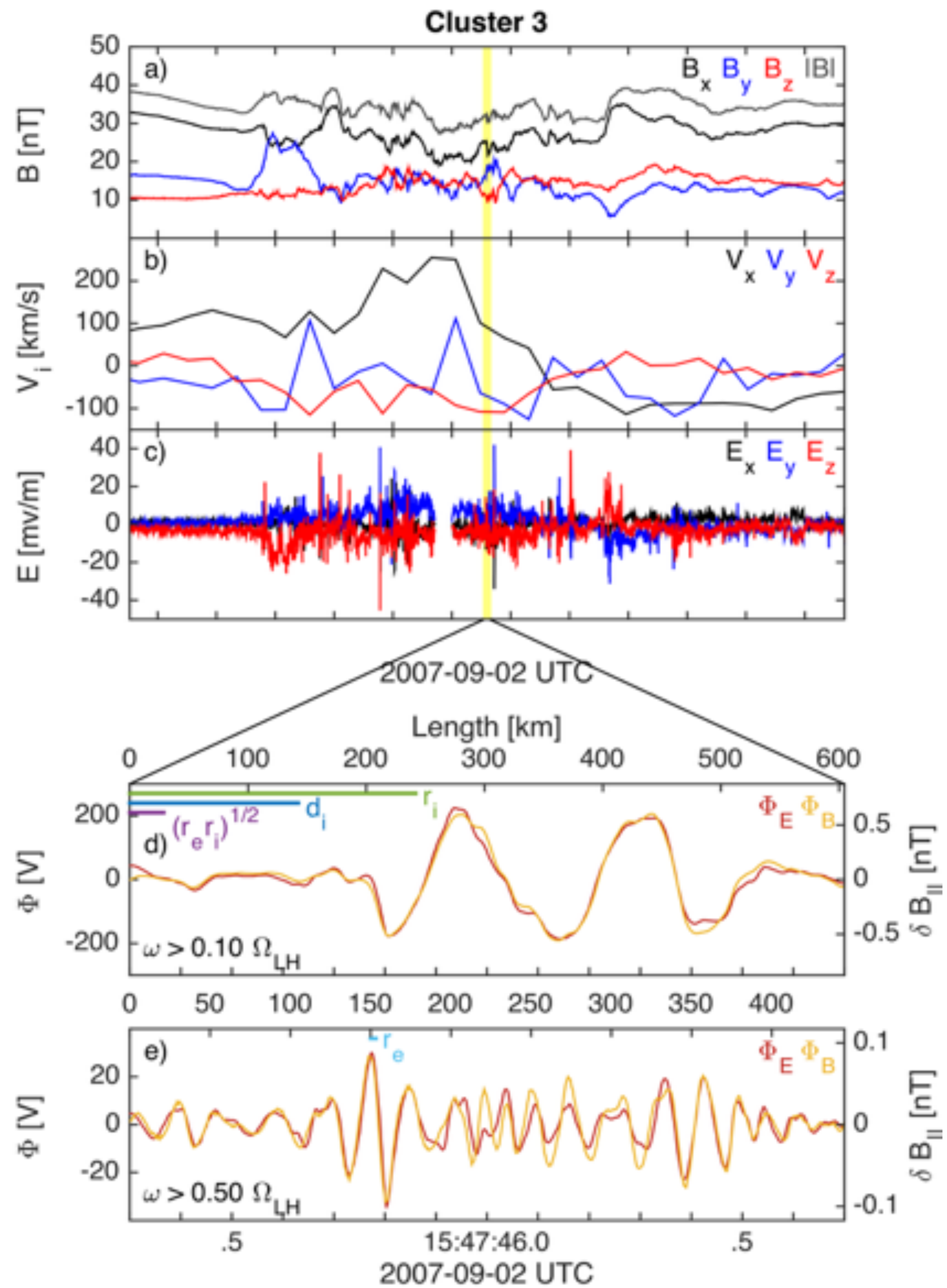

Credit: Cecilia Norgren, University of Uppsala

$\lambda \sim 150$ km$= 5.5\sqrt{(\rho_e \rho_i)}$
→ EM branch

$\lambda \sim 27$ km$= 7\ \rho_e$
→ ES branch

Conclusions

- The Multi-Level Multi-Domain method is a fully kinetic, semi-implicit adaptive method to reduce the cost of Particle In Cell Implicit Moment Method plasma simulations; we target in particular realistic mass ratio simulations

- the MLMD method has been demonstrated in two kinds of scenarios:
  1. problems where small scale, high frequency processes are confined in a small portion of the entire domain e.g.: magnetic reconnection
  2. self-similar processes where only a representative part of the domain is simulated with higher resolution e.g.: Lower Hybrid Drift Instability

- in both cases, the physical processes of interest are correctly reproduced, at a lower computational cost

- during the *Hands On*: verify the multi scale nature of collisionless magnetic reconnection, as simulated with iPic3D